Rotational Dynamics of Coumarin 153: Time-Dependent Friction, Dielectric Friction, and Other Nonhydrodynamic Effects

M.-L. Horng, J. A. Gardecki, and M. Maroncelli*

Department of Chemistry, 152 Davey Laboratory, The Pennsylvania State University, University Park, Pennsylvania 16802

Received: September 23, 1996; In Final Form: November 14, 1996[⊗]

Subpicosecond fluorescence anisotropy measurements are used to characterize the rotational dynamics of coumarin 153 (C153) in 35 common solvents and eight solvent mixtures at room temperature. The rotational anisotropy decays of C153 are generally nonexponential as a result of the non-Markovian nature of the friction on its rotational motion. Rotational correlation times are observed to be larger in polar solvents than in nonpolar solvents of the same viscosity. This difference is examined in the context of theories of dielectric friction, which relate the extra friction in polar solute/solvent systems to long-range dipole−dipole interactions. Since the latter interactions have been thoroughly characterized via dynamic Stokes shift measurements for the same solute/solvent combinations studied here, the present data provide a unique opportunity to test general concepts of dielectric friction. Contrary to expectations, the departures from simple hydrodynamic behavior cannot be modeled using only theories of rotational dielectric friction. More important than dielectric friction is the role that the relative solute/solvent size plays in determining the extent of solute−solvent coupling. Once this size dependence is approximately accounted for, the remaining departures from simple hydrodynamic behavior are relatively small in all solvents. In polar aprotic solvents, solvation data indicate that dielectric friction effects should be rather modest (10−20% of the total friction). In these solvents no clear correlation is found between dielectric friction predictions and the observed solute−solvent coupling. However, in normal alcohol solvents the effects of dielectric friction are predicted to be large and well beyond the scatter in the experimental data. No evidence for such an important dielectric friction contribution is observed in these solvents, in spite of the fact that long-time components of the solvation dynamics do appear to be present in the rotational friction.

I. Introduction

The nature of rotational motion in solution has been a subject of long-standing interest in physical chemistry because such motions directly reflect the interactions between a solute molecule and its solvent surroundings.[1−4] For this reason, studies of rotational dynamics provide a useful starting point for exploring the nature of solvent friction and how it influences more complex dynamics such as chemical reaction.[5] Since our understanding of many aspects of solution phase dynamics has grown impressively over the past decade, it may seem surprising that our understanding of friction in even the simple case of solute rotation is still far from quantitative. To be sure, some aspects of solvent friction can be easily understood in terms of hydrodynamic theories, which derive from extrapolating the behavior of macroscopic objects down to the molecular level. The Stokes−Einstein−Debye (SED) model of rotational motion, proposed well over half a century ago,[6] is such a theory. It associates molecular-level friction with bulk viscosity in such a way as to provide reasonable estimates of the rotation times of molecules in solution. However, the coupling between a solute and its surroundings cannot be quantitatively described solely in terms of macroscopic hydrodynamics. Experimental data on even relatively large solutes often show characteristic departures from hydrodynamic predictions. It is such deviations from the SED (and related) theories that are the focus of most interest, for it is through these deviations that molecular aspects of the solvent−solute coupling are revealed. While the experimental data on such deviations have been steadily accumulating, our ability to quantitatively predict how molecular aspects of solute−solvent interactions cause these deviations is still rather meager.

The present paper reflects an attempt to improve this situation by providing an extensive set of data on the rotational dynamics of a relatively simple polar solute, coumarin 153 (C153). Our

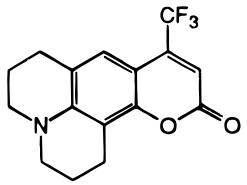

Coumarin 153

primary focus will be on exploring how electrical aspects of the solute−solvent coupling, know as "dielectric friction", cause deviations from simple hydrodynamic behavior. In particular, we employ the information recently acquired on polar solvation dynamics of this probe in order to explore how dielectric friction influences its rotational motion. By doing so, we are able to draw some fairly general conclusions about the relationship between solvation and the electrical component of the friction on polar solutes. In addition, the broad range of solvents examined here also allows for some interesting conclusions regarding other nonhydrodynamic aspects of rotational friction of relevance to both polar and nonpolar solutes.

The outline of the remainder of this paper is the following. In section II we describe the theoretical background necessary to our analysis and provide some perspective on previous experimental investigations of rotational dielectric friction. Although we do not review all of the experimental work in

[⊗] Abstract published in *Advance ACS Abstracts,* January 1, 1997.

S1089-5639(96)02921-0 CCC: $14.00

detail, the references provided in this section are relatively complete. To measure rotational dynamics here, we employ the fluorescence up-conversion technique, which enables the rotational motion of the excited state of C153 to be observed with subpicosecond time resolution. The apparatus and methods of data analysis are described in section III. The main results of this work are then presented in four parts. In section IVA we describe the nature of the emission anisotropies observed with C153. These anisotropies are generally nonexponential functions of time. We show how this nonexponentiality can be related to the time dependence of the friction on rotational motion. Section IVB then considers (average) rotation times and how these times vary with solvent. We find that there is a marked difference between the rotation times measured in polar versus nonpolar solvents, with rotation being considerably slower in polar solvents for a given viscosity. We first attempt to associate these differences with the effect of dielectric friction on the rotational motion, using the general connection to solvation dynamics established by van der Zwan and Hynes.[7] The failure to find any satisfactory correlation to dielectric friction predictions then leads us to consider other nonhydrodynamic effects on the rotational motion in section IVC. There we show that variations in the rotational coupling caused by variations in the sizes (and shapes) of solvent molecules are at least as important as dielectric friction effects in causing the different rotational dynamics in polar and nonpolar solvents. Once this size dependence is approximately accounted for, we again look for the signatures of dielectric friction in section IVD. In polar aprotic solvents, we find that if dielectric friction effects are indeed present, they are masked by larger solvent size/shape effects. In normal alcohol solvents, where solvation data imply large and readily measurable dielectric friction effects, we observe none. Finally, section V presents a summary and comparison to past work as well as some comments on the apparent lack of dielectric friction effects in this system.

II. Theory/Background

A. Basic Hydrodynamic Theory and Dielectric Friction. Nearly all analyses of experimental rotational data begin with the Stokes−Einstein−Debye (SED) model. Assuming that molecular rotation is analogous to motion of a sphere of volume V_p in a continuous fluid of shear viscosity η, Debye derived the result

$$\tau_{rot}^{(1)} = \frac{\zeta}{2k_BT} = \frac{6V_p\eta}{2k_BT} \tag{1}$$

where k_BT is Boltzmann's constant times the temperature. Minor modification of this equation serves to bring it into the form commonly used to analyze experimental data:[8,9]

$$\tau_{rot}^{(L)} = \frac{\zeta}{L(L+1)k_BT} = \frac{6V_pf\eta}{L(L+1)k_BT}C \tag{2}$$

In this expression L is the rank of the orientational correlation function considered ($L = 2$ for the experiments described here), and f is a factor that accounts for the nonspherical shape of the solute. This solvent-independent constant can be reliably calculated using results on ellipsoidal bodies derived by Perrin.[10] Finally, the factor of C in eq 2b can be considered a "coupling parameter"[11] which serves as an overall correction for deviations from the basic SED predictions.

The remarkable success of this simple hydrodynamic theory results from its prediction that rotation times should be proportional to the ratio η/T. When measurements are made within a single solvent, this proportionality (or something close to it[8]) is indeed observed in nearly all cases.[2−4,12] Such a result is not surprising, since such a proportionality to η/T is expected on rather general grounds.[13] What is perhaps more surprising is that the actual rotation times predicted by SED theory are often comparable to measured rotation times. That is, the proportionality constant, which was derived by considering only the behavior of a macroscopic body in a continuous fluid, is not too far from molecular reality. To the extent that this is the case, measurements of rotational dynamics teach us no more about the details of frictional interactions in solution than do viscosity measurements. However, more often than not, the quantitative predictions of the simple hydrodynamic theory (i.e., eq 2 with $C = 1$) are incorrect by a considerable amount. In addition, it is very often found that while rotation times may be proportional to η/T in a single solvent, the proportionality constant varies considerably from solvent to solvent. Especially in the latter case, empirical values of the "coupling parameter" C, defined by

$$C_{obs} = \frac{L(L+1)k_BT}{6fV_p\eta}\tau_{obs}^{(L)} \tag{3}$$

may serve to point out how the frictional forces on a molecular solute differ from those operating on a macroscopic object.[11]

Variants of the basic hydrodynamic theory can provide some insight into the meaning of this coupling parameter. Even using a continuum description of the solvent, it is possible to choose different boundary conditions for solving the hydrodynamic equations, and C can be viewed as varying with this choice.[14−17] The original SED equation ($C = 1$) presupposes a "stick" boundary condition wherein the fluid layer immediately adjacent to the solute is assumed to move with the same velocity as the solute. But the concept of an infinitesimal fluid layer has no precise meaning relative to a molecular solute rotating in a solvent consisting of comparably sized molecules. Thus, strict application of such a boundary condition is not expected to yield an appropriate coupling constant. Indeed, a "slip" boundary condition (zero tangential velocity of the fluid layer adjacent to the solute) may be a more useful first approximation, especially in the case of small solutes.[3,18,19] For a spherical solute, slip boundary conditions imply no friction on rotation ($C = 0$). For nonspherical solutes, the value of C predicted by a complete hydrodynamic calculation is a sensitive function of solute shape, ranging anywhere between zero and unity.[14,15] In addition, hydrodynamic boundary conditions intermediate between the slip and stick limits can also be examined.[16] All of these possible variants lead to a great deal of latitude in the hydrodynamic predictions for C. What one can say generally is that whatever boundary conditions are applied, the hydrodynamic prediction for C will approach unity (i.e., the stick prediction) the more "knobby" the solute shape.[17,18] Thus, in some sense, hydrodynamic models can be used to rationalize the values of C observed empirically.

However, even allowing for the possibility of different boundary conditions, purely hydrodynamic models are far from adequate to describe the range behavior observed in experiment. In many instances either "subslip" or "superstick" values of C are observed.[2−4] More importantly, for a given solute, the value of C is often found to vary significantly with solvent. For example, Ben-Amotz and co-workers have nicely documented the fact that polyaromatic hydrocarbons have much smaller values of C_{obs} in alcohols compared to other solvents.[20] Clearly, such behavior cannot be accounted for by any theory which models the solvent as a viscous continuum. Descriptions that

include more details of the solute−solvent coupling are required. Unfortunately, whereas experimental information on deviations from simple hydrodynamic behavior is plentiful,[2−4,20] theories that adequately describe such deviations are relatively few in number.

Theories that go beyond a purely hydrodynamic description of rotation can be classified into two main categories. The first category consists of theories that explore what role the finite size of solvent molecules plays in determining the frictional coupling. These include theories that begin with rigorous kinetic theory results[21−23] as well as the more heuristic approaches of Geirer and Wirtz[24] and Dote, Kivelson, and Schwartz.[25] While the former theories are perhaps more solidly grounded, they tend to be difficult to apply to experimental situations. (Nevertheless, Ravi and Ben-Amotz[26] have recently made insightful comparisons between experiment and the kinetic theories of Evans and co-workers.[23]) We will have more to say about the theories of Geirer and Wirtz and Dote *et al.* in section IVC. For now, we simply point out that these theories predict that the coupling parameter should decrease as the relative solvent/solute size ratio increases, as which is observed in the present experiments.

Of more direct interest in the present study are a second general class of models, which relate deviations from simple hydrodynamic behavior to the presence of additional mechanisms of friction not accounted for in the hydrodynamic descriptions. One limiting case of such models can be termed "solventberg" pictures,[27,28] applicable when long-lived, specific associations exist between the solute and solvent. The idea behind such models is simple. If one or more solvent molecules remain attached to the solute over the course of a rotational period, it is natural to modify C_{obs} so as to incorporate the entire volume of the supramolecular assembly that is actually rotating. The rotation of this assembly then takes place through the surrounding "unbound" solvent, which can be adequately treated via hydrodynamic theories. This solventberg approach should be most useful in the case of small ionic solutes or in cases where strong hydrogen bonds are present between the solvent and solute. But, as we will discuss later, the presence of solute−solvent hydrogen bonding does not necessarily imply that such a description will be valid.

Nonspecific interactions can also lead to deviations from hydrodynamic behavior, by virtue of an effect termed "dielectric friction". It is this final source of nonhydrodynamic behavior that is the main focus of the present work. The nature of dielectric friction can be described in the following way. In purely hydrodynamic theories it is assumed that the frictional coupling between a solute and solvent depends only on the solute shape and the solvent viscosity. Such theories therefore predict that polar and nonpolar solutes of identical shape will feel identical friction in any solvent of a given viscosity. But this prediction cannot be completely correct. In a polar solvent, an increase in solute polarity (i.e., an increase in the charge on solute atoms) necessarily implies an increase in the magnitude of solvent−solute interactions and thus in the friction it will experience. The "extra" friction due to electrostatic interactions is what is referred to as dielectric friction. This friction is generally assumed to simply add to the friction due to other sources:

$$\zeta_{tot} = \zeta_{hyd} + \zeta_{el} \tag{4}$$

In this expression ζ_{hyd} is the "hydrodynamic" or "mechanical" component of friction, assumed to be described by eq 2, and ζ_{el} is the electrical or dielectric component of the friction. Since the latter is not necessarily proportional to solvent viscosity, the dielectric friction component, rather than altering C, actually allows for a part of the friction that does not follow an η/T law.

A number of theories of rotational dielectric friction have been proposed,[29−38] beginning with the seminal work of Nee and Zwanzig.[30] All of these theories share two basic assumptions about the nature of dielectric friction. The first is that the separation of friction due to electrical interactions and other "hydrodynamic" interactions in eq 4 is valid.[39] (Molecular dynamics simulations show that this assumption may be incorrect in the case of small, highly polar solutes.[40]) The second assumption is that the polarization response which leads to dielectric friction is linear in the magnitude of the solute charges. From these basic ideas, most theories go on to make predictions concerning the magnitude of the dielectric friction by modeling the polarization response of the solvent with dielectric continuum approaches. For example, the Nee−Zwanzig theory predicts that, for a solvent with a Debye dielectric response, the dielectric friction component should be given by[30,41]

$$\zeta_{el} = \frac{2\mu^2}{a^3} \frac{(\epsilon_\infty + 2)^2(\epsilon_0 - \epsilon_\infty)}{3(2\epsilon_0 + \epsilon_\infty)^2} \tau_D \tag{5}$$

In this expression μ and a are the dipole moment and radius of the solute (assumed spherical), and ϵ_0, ϵ_∞, and τ_D are parameters specifying the dielectric response of the solvent. The Nee−Zwanzig theory and several more sophisticated theories of dielectric friction have been recently reviewed and tested against computer simulation results on simplified dipole lattice model solvents in ref 42. At least for such idealized solvents, it was found that continuum dielectric predictions for solvation and friction are rather inaccurate. In this case, molecularly based models of solvent−solute interactions were found necessary in order to achieve acceptable agreement with simulation results.[42] However, recent experimental studies indicate that these same dielectric continuum predictions do in fact provide reasonable estimates for the solvation behavior of real-world solvents.[41]

But examination of dielectric friction need not be tied to any particular model of solvation. Using only the basic ideas outlined above,[43] it is possible to show that the dielectric component of rotational friction should be closely related to another experimentally observable phenomenon, "polar solvation dynamics".[44] The term solvation dynamics refers to the time-dependent change in the electrical component of the solute−solvent interaction energy subsequent to some perturbation of the solute's charge distribution. This dynamic can be observed by monitoring the time-dependent shift in the emission frequency of a suitable solvatochromic probe subsequent to electronic excitation.[44] The relationship between dielectric friction and solvation dynamics is most simply displayed by assuming that the solute charge distribution can be represented by a point dipole moment. In this case the fluctuating torques that are responsible for the dielectric component of the friction can be easily related to the time-dependent fluctuations in the electrical field the solvent imposes on the dipole (μ).[7,41,42] Assuming a linear solvent response, these same electric field fluctuations also determine the time-dependent response to a change in the dipole moment of the solute ($\Delta\mu$). van der Zwan and Hynes[7] were the first to show that the time-dependent spectral shift observed subsequent to exciting such a dipole change in a solute is simply proportional to the time-dependent dielectric friction on its rotational motion. These authors derived what we will refer to as the "van der Zwan−Hynes" connection:

$$\zeta_{el}(t) = \left(\frac{\mu^2}{(\Delta\mu)^2}\right)\{hc\Delta\bar{\nu}S_\nu(t)\} \quad (6)$$

In this expression $hc\Delta\bar{\nu}$ is the magnitude of the shift of the emission spectrum (expressed in energy units), and $S_\nu(t)$ represents the normalized time dependence of this shift.[44] The dielectric friction function $\zeta_{el}(t)$ that appears here is related to the (integral) friction constant normally encountered in rotational problems via

$$\zeta_{el} \equiv \int_0^\infty \zeta_{el}(t)\,dt = \left(\frac{\mu^2}{(\Delta\mu)^2}\right)\{hc\Delta\bar{\nu}\tau_\nu\} \quad (7)$$

where τ_ν is the integral time associated with $S_\nu(t)$. While the above expressions are derived on the basis of a point dipole approximation for the solute charge distribution, one would expect the proportionality $S_{el}(t) \propto \Delta\nu S_\nu(t)$ should hold at least approximately even without this simplification.

B. Experimental Study of Rotational Dielectric Friction. Over the past decade, a number of experimental studies of the rotational dynamics of charged and dipolar solutes have been examined in light of dielectric friction concepts.[45−63] While there now exists a considerable database of high-quality rotation data, no definitive understanding of how dielectric friction influences solute rotation has yet emerged. The reason is that interpretation of experimental data in terms of dielectric friction ideas is confounded by three difficulties. First, it is not easy to distinguish between the effects of specific association (solvent-berg formation) and the influence of nonspecific dielectric interactions.[64] Part of the problem is that, for reasons of experimental convenience, most of the solutes examined to date have been charged molecules[45−51,55,56,58−60] or molecules with hydrogen-bond-donating groups that may be expected to form specific associations with many solvents.[52,61] For example, one of the most thoroughly studied solutes is the anionic dye "resorufin". No fewer than five distinct research groups have examined this solute in a wide variety of solvents.[28,47,50,59,60,65] Especially in alcohol solvents, the interpretations placed on the observed rotation times cover a complete spectrum of possibilities, ranging from a highly detailed picture of specific attachment of a solvent molecule to each end of the solute[28] to application of the point dipole/dielectric continuum description of Nee and Zwanzig.[50] To narrow this wide range of possible interpretations, careful selection of solute/solvent combinations is necessary. In an attempt to focus on nonspecific dielectric effects, many of the more recent studies have employed uncharged solutes with no obvious hydrogen-bond-donating groups.[53,54,57,62,63] However, even here specific interactions may still play an important role in some solvents. Alcohols are a case in point, since virtually any polar solute is likely to have sites available for possible coordination of a hydrogen-bond-donating solvent. Yet most experimental studies of dielectric friction have in fact made extensive use of alcohol solvents, for the simple reason that only in such solvents does one predict large nonspecific dielectric friction effects. Thus, the experimentalist faces the dilemma that the solute/solvent combinations that are expected to lead to the most readily observable effects are also those wherein this effect is least clearly interpreted.

A second difficulty that complicates interpretion of rotation data is the need to isolate the influence of dielectric friction from other nonhydrodynamic effects. Most experimental studies of dielectric friction have compared rotation times of a single solute in a series of solvents of varying dielectric properties. Differences in C_{obs} between a given solvent and some reference solvent with negligible dielectric friction (typically alkanes for neutral solutes[53,62] or water for charged solutes[50,51]) are then used to measure the extent of dielectric friction. However, use of reference solvents in this way is not straightforward. As we will show later, nonhydrodynamic effects related to the sizes and shapes of solvent molecules may contribute to differences between C_{obs} in different solvents in a way that may be difficult to predict or control. Extraction of the dielectric friction contribution within a single solvent can also be accomplished by comparing two or more solutes whose shapes are similar but whose electrical properties differ. Waldeck and co-workers have attempted several comparisons of this sort with charged[59,60] and uncharged solutes.[61−63] However, just as with solvent variation, since chemically distinct solutes cannot have identical molecular shapes, it is once again difficult to assess how much differences other than the electrical ones of interest contribute to changes in the solute−solvent coupling one observes. The cleanest way to get around this difficulty is to measure the rotation times of a single solute in both its ground and electronically excited states. If there is no conformational change upon excitation, it is reasonable to expect that the shape of the solute is unchanged in the process and that therefore any differences in solute−solvent coupling can be ascribed solely to changes in the electrical interactions between the solvent and the two different solute charge distributions. Thus far, comparatively few of these sorts of measurements have been made, and unfortunately all of them have involved ionic or hydrogen-bond-donating solutes.[48,52,64,59,60] More work along these lines, especially with simple dipolar solutes, would be highly desirable.

A final source of ambiguity in testing dielectric friction ideas involves the methods used to predict the magnitudes of the effects expected. The majority of experimental studies to date have employed theories like the Nee−Zwanzig theory,[30] which rely on point dipole solute/dielectric continuum solvent descriptions.[45−56] The adequacy of such simplistic models for predicting the electrical component of solvent−solute interactions is not clear. First, the representation of the solute as a spherical point dipole is suspect. As an improvement on the basic model Alavi and Waldeck recently developed an extension of the Nee−Zwanzig formalism that treats the case of an extended charge distribution within a spherical cavity.[35] They showed that higher moments of the solute's charge distribution can dramatically increase its interactions with a continuum solvent relative to the case of a centered point dipole alone. Waldeck and co-workers have applied this idea to successfully rationalize the rotation times observed in a number of solutes.[66,60−63] But whether this distributed charge approach is actually more accurate than the original Nee−Zwanzig approach is not known. In both cases the magnitudes of the electrostatic interactions are highly sensitive to the choice of a cavity radius, and this choice is far from obvious when it comes to the sorts of solutes studied in experiment. In addition, the *dynamics* of the electrical interactions are not always captured adequately by continuum solvent models.[41] To avoid possible inaccuracies inherent in cavity solute/continuum dielectric models, a number of recent studies have instead employed various forms of the the van der Zwan−Hynes relationship (eq 7).[49,57,58−61] Thus far, workers have measured some approximation to the magnitude of the solvation-induced shift $\Delta\bar{\nu}$ for the solute of interest and then used solvation times computed on the basis of dielectric data and continuum dielectric models of solvation. Clearly, a more exacting test of this connection would be to measure both $\Delta\bar{\nu}$ and τ_ν with the solute whose rotational dynamics is being examined.

Due to the difficulties enumerated above, and in spite of a substantial experimental effort, the influence of nonspecific

dielectric friction on solute rotation has yet to be unambiguously demonstrated. To do so would require an "ideal" experiment incorporating the following features. First, the solute chosen for study should be uncharged and have no hydrogen-bond-donating sites. In this way the possibility of specific association could be eliminated, at least in polar aprotic solvents. Second, rotation times in both the ground and excited state would need to be measured, so that their difference could be used to accurately determine the magnitude of the dielectric friction effect. Finally, the solvation dynamics of this same solute would have to be measured in order to enable complete use of the van der Zwan−Hynes relationship. Such an experiment would allow for a true test of the basic ideas that underly all theories of dielectric friction. In the present work we report a new set of rotational meaurements in which most, but unfortunately not all, of the above requirements are fulfilled.

III. Experimental Section

Coumarin 153 (Exciton, laser grade) was used as received. Solvents (Aldrich, HPLC or spectral grade) were used without further purification, with the exception of dimethylformamide (DMF), which was fractionally distilled and dried over molecular sieves. To obtain nonpolar solvents with viscosities comparable to those of the normal alcohols, mixtures of hexanes and squalane (2,6,10,15,19,23-hexamethyltetracosane) were prepared volumetrically.

Steady-state anisotropies were measured in propylene glycol using a Spex Fluorolog F212 spectrometer. The samples ($\sim 5 \times 10^{-5}$ M) were placed in 1 cm path length cuvettes and then vacuum-sealed with a removable Teflon fitting. The sealed cuvettes were enclosed in a copper compartment attached to the cold finger of an Oxford Instruments DN 1754 liquid nitrogen cryostat, which maintained a temperature of 200.0 ± 0.2 K during the measurements. Polarized excitation spectra were corrected for the response of the detection system to each polarization component (*G* factor) as described in ref 67. The wavelength-dependent *G* factor was determined by averaging four emission scans. As a check, the fluorescence anisotropy of perylene was also measured in propylene glycol at 200 K, and the results were found to be within uncertainties of those previously reported by Shinitzky *et al*.[68]

Viscosities of the solvents employed here were mostly obtained from the compilations of Riddick *et al*.[69] The main exceptions were the nonpolar solvent mixtures, which were instead measured with a calibrated routine viscometer (Cannon-Fenske 75 K60) thermostated in a water bath at 25.0 ± 0.1 °C. These measured viscosities were reproducible to within ±1%. Their accuracy was assessed by measuring the viscosities of several well-studied solvents. The viscosities of hexane, decalin, and ethylene glycol measured here were 0.311, 2.31, and 16.5 cP, respectively, which agree with literature values (0.294, 2.415, and 17.3 cP[69]) to within about ±5%.

Time-resolved fluorescence anisotropies were measured using a femtosecond up-conversion apparatus which has been described in detail in ref 70. Briefly, an unamplified Ti:sapphire laser system (Coherent Mira 900F) provided output pulses of ∼70 fs duration at a wavelength of ∼774 nm and repetition rate of 76 MHz. Light of the doubled frequency, generated by type I mixing in a 0.2 mm BBO crystal, was used for exciting the sample. The second harmonic was separated by a dichroic beam splitter and compressed by a prism pair. The polarization of the compressed excitation pulses was controlled by a half-wave plate prior to focusing into a flowing sample cell with a sample thickness of 1 mm. Samples for these experiments consisted of concentrations of C153 of between 7×10^{-5} M (alkane solvents) and 5×10^{-4} M (other solvents). The temperature was 22 ± 2 °C. The forward-scattered fluorescence was collected and focused into a 0.4 mm BBO crystal by an elliptical reflector. The residual fundamental beam (vertically polarized) was subjected to a variable delay and focused into the same BBO crystal with a 100 mm focal length lens to serve as the gate pulse for up-converting the sample emission. The up-converted light produced by type I phase matching in the BBO crystal was detected with a photomultiplier tube and digitized by a photon counter. The overall instrumental response of this system was typically 120 fs as judged by the full width at half-maximum of the cross-correlation between the pump and gate pulses.

The polarization of the pump beam with respect to the gate beam was controlled by a half-wave plate in the pump arm. For anisotropy measurements, the half-wave plate was rotated between the vertical and horizontal positions to measure parallel $I_{||}(t)$ and perpendicular $I_{\perp}(t)$ signals. The polarization purity of the pump beam was 99.8% as determined by measuring its extinction through crossed polarizers. The polarization of the up-converted signal was also confirmed to be better than 99.8%, as judged by the relative intensities of cross-correlation signals measured with vertical and horizontal excitation. Using type I phase matching and vertical polarization of the gate beam, only the vertical component of the fluorescence is up-converted. Hence, the polarization characteristics of the up-converted signal are independent of the polarization of the excitation beam. The relative sensitivities for detecting $I_{||}$ and $I_{\perp}$ (the "*G*" factor) should therefore be unity in these experiments. Comparison of signals at times long relative to anticipated rotation times ("tail matching") did indeed show an average *G* value of 1.02 ± 0.03.

Collection of a set of anisotropy data consisted of measuring fluorescence decays at parallel, magic angle (54.7°), and perpendicular polarizations. A single decay measurement entailed of an average over two scans, each of which employed multiple step sizes of 0.02, 0.2, 2, and 10 ps. Fluorescence over a total span of 200, 800, or 1100 ps was collected depending on the rotation times expected in a given solvent. In polar solvents, the fluorescence of C153 at a given wavelength may rise or decay rapidly due to the time-dependent Stokes shift of the emission spectrum. While this dynamics did not produce an observable effect on the anisotropies measured (see section IVA), anisotropies were generally measured at the particular wavelength for which the emission decays showed no fast rise or decay behavior (typically $480 \leq \lambda_{em} \leq 510$ nm in polar solvents).

Since the rotational time scales observed here are much slower than the instrumental response, time-resolved fluorescence anisotropies, $r(t)$, were directly calculated from the parallel and perpendicular decays without deconvolution. In a variety of test cases, iterative reconvolution fits, which largely remove the effects of instrumental broadening, gave identical results to this direct method of analysis. The time shift obtained from a recovolution fit to the fluorescence decay at the magic angle was used to determine the time origin. In calculating the anisotropy decays, account was made for the (small) differential sensitivity to the two polarizations (*G*) and a constant background contribution (*b*) by using the form

$$r(t) = \frac{I_{||}(t) - GI_{\perp}(t)}{I_{||}(t) + 2GI_{\perp}(t) - 3b} \tag{8}$$

The *G* factor was obtained by tail matching up-converted signals $I_{||}(t)$ and $I_{\perp}(t)$, and the base line (*b*) was determined by the signal

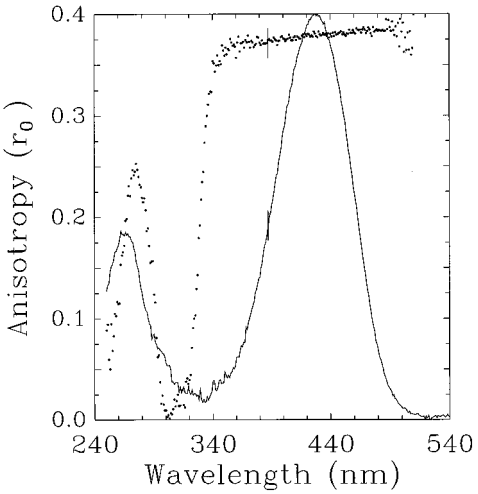

Figure 1. Steady-state absorption (solid curve) and excitation anisotropy (points) spectra of C153 in propylene glycol at 200 K. The vertical line through the anisotropy data marks the excitation wavelength (387 nm) used in the time-resolved measurements.

level at $t < 0$. In addition to $r(t)$, the isotropic intensity

$$I_{iso}(t) = \frac{I_{||}(t) + 2I_{\perp}(t)}{3} \tag{9}$$

was also calculated. Comparing this computed isotropic decay to the experimentally measured magic angle decay provided a check for errors introduced by laser power instabilities, changes in sample fluorescence, degradation of sample, or drift of the detection system. Cases in which the two did not agree to better than ±5% were rejected.

IV. Results and Discussion

A. Time-Resolved Anisotropies and Time-Dependent Friction. In order to estimate the initial anisotropy $r(t = 0)$ to be expected in the time-resolved experiments, we first examine the steady-state anisotropy of C153 in a glassy solvent, propylene glycol at 200 K. The steady-state excitation anisotropy (emission observed at 555 nm) is shown in Figure 1. As can be seen from this figure, the excitation anisotropy of C153 is nearly constant over the region of the lowest frequency absorption band. This constancy, and the fact that $r_0 \sim 0.4$, the limiting value for parallel absorption and emission dipoles underscores the simplicity of the S_1 spectrum of C153.[71] Between 353 and 486 nm (the points where the S_1 absorption has dropped to 10% of its maximum value), the steady-state anisotropy is well fit by the linear relation $r_0 = 0.3267 + 1.206 \times 10^{-4}\lambda$ (nm). At the excitation wavelength employed here (387 nm), the value of r_0 is 0.373 ± 0.005, which corresponds to an angle of 12° between the absorption and emission transition moments. For judging the initial anisotropy expected in a given solvent, some account must be made for the fact that the absorption spectrum of C153 shifts systematically as a function of solvent polarity. If we assume that r_0 in a given solvent depends only on the relative position of λ_{ex} within the absorption profile, the values of r_0 are expected to vary between 0.378 in nonpolar solvents and 0.373 in the most polar solvents. This change with excitation wavelength is relatively small. It therefore seems reasonable to simply assume that $r(t=0)$ should lie within the range 0.374 ± 0.008 in all solvents.

Representative time-resolved decays of C153 in hexamethylphosphoramide (HMPA) are shown in Figure 2. The unusual appearance of this "raw" data stems from the use of multiple step sizes in data collection. Multiple time-step scans are

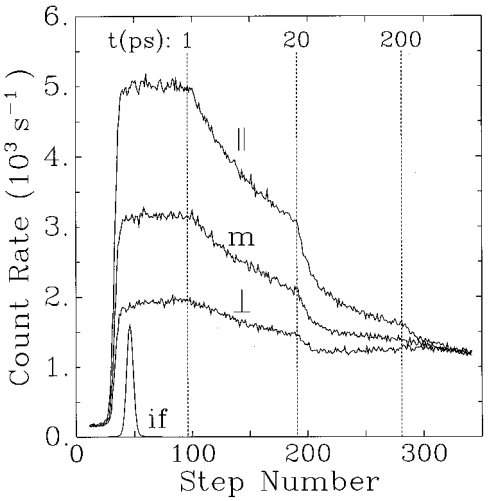

Figure 2. Representative parallel (||), magic (m), and perpendicular (⊥) emission decays of C153 in HMPA ($\lambda_{em} = 490$ nm). Also shown is the instrumental response function (if), which is the cross-correlation between the excitation and gate pulses. The vertical lines and the times indicated at the top of the figure denote the points at which the sampling interval changes. The intervals used here are 20 fs before 1 ps, 200 fs before 20 ps, and 2 ps before 200 ps and 10 ps between 200 and 800 ps.

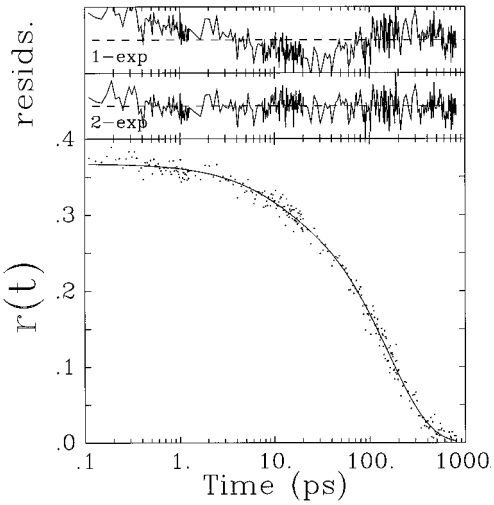

Figure 3. Example of an emission anisotropy decay fitted by single-exponential and biexponential functions. Data are for C153 in HMPA. The points shown in the bottom panel are the $r(t)$ values calculated from the decay data in Figure 2 using eq 8. The solid curve through these points represents the biexponential fit to the $r(t)$ data (eq 10). The two top panels are the residuals of the single-exponential (top) and biexponential (middle panel) fits. The fit parameters in these examples are as follows. 1-exp: $r(0) = 0.350$, $\tau_1 = 137$ ps, $\chi_\nu^2 = 2.1$; 2-exp: $r(0) = 0.367$, $a_1 = 0.13$, $\tau_1 = 9.1$ ps, $\tau_2 = 157$ ps, $\chi_\nu^2 = 1.0$.

essential when highly dispersive kinetics, such as occur in solvation dynamics, are studied.[70] In the present context, we have found that collecting data in this manner is also helpful for observing nonexponentiality in $r(t)$, as discussed below. After checking for consistency between the isotropic decay (calculated from eq 9) and the observed magic angle decay, anistropies were constructed from $I_{||}(t)$ and $I_{\perp}(t)$ according to eq 8. Typical $r(t)$ functions are provided in Figures 3 (HMPA) and 4 (1-pentanol).

Before discussing the analysis of such data, we digress momentarily to point out that the emission of C153 differs from that of most other probes used to study rotational dynamics. Since the spectrum of C153 undergoes a time-dependent shift of ~2000 cm^{-1} in polar solvents, even emission collected at the magic angle is often highly nonexponential. For example,

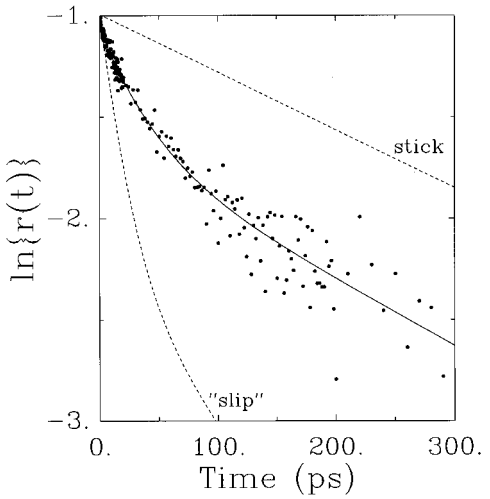

Figure 4. Rotational anisotropy data (points) and fit (solid curve) for C153 in 1-pentanol at 295 K. The solid curve through these points represents the biexponential function: $r(t) = r(0)\{0.446 \exp(-t/31.6 \text{ ps}) + 0.554 \exp(-t/405 \text{ ps})\}$, with $r(0) = 0.378$. The dashed lines are the results of hydrodynamic calculations based on an ellipsoidal model of the solute and stick and slip boundary conditions (see section IVB).

the magic angle curve in Figure 2 shows a drop of roughly 50% over the first 200 ps, even though the emission lifetime is ∼5 ns in this solvent. It is important to consider whether this spectral movement or the underlying solvation process that it reflects has any direct bearing on the anisitropy decays being measured. Some indication of a direct coupling between solvation dynamics and rotational motion was recently provided by Khundkar and co-workers.[57] They reported a systematic variation in the emission anisotropy decay times measured at different emission wavelengths with the highly solvatochromic probe *p,p′*-cyanothiomethyldiphenylacetylene in 1-propanol.[57] In our original study of the probe C153,[72] no such differences were observed. However, to confirm this result, we once again examined whether there was any wavelength dependence to the anisotropy data. In the three solvents methanol, acetonitrile, and dimethyl sulfoxide we measured anisotropy decays at emission wavelengths of 480, 540, and 505 nm, wavelengths which approximately correspond to the frequencies half-height and peak positions of the steady-state emission spectrum. (See ref 70 for representative spectra.) The results confirmed the conclusions of the previous study. In none of these three solvents did the anisotropies measured at different wavelengths show any systematic variation of either the $r(0)$ values (>2%) or time constants (>5%) of the $r(t)$ decays. Thus, the anisotropy decays measured here are not directly affected by the spectral/solvation dynamics also occurring when one excites C153.

We now return to the analysis of the $r(t)$ data. These data were fit to the biexponential function

$$r(t) = r(0)\{a_1 \exp(-t/\tau_1) + (1 - a_1) \exp(-t/\tau_2)\} \quad (10)$$

using a nonlinear least-squares algorithm. Examples of such fits for the HMPA case are provided in Figure 3. The noise in the $r(t)$ data shown here is representative of the signal-to-noise (S/N) ratios typically observed in these experiments, which was ±3−10% of $r(0)$, depending on solvent. To avoid artifacts due to instrumental broadening, only data at times greater than 0.2 ps were included in the fitting procedure. A given data set was first fit to a single-exponential form ($a_1 = 1$) with values of $r(0)$ and τ_1 freely varied. The fit was considered acceptable if the resulting value of $r(0)$ was within the expected range (0.366−0.382), the χ_ν^2 statistic[73] was close to unity, and the residuals showed no clearly nonrandom pattern. In roughly half of the solvents examined here a single-exponential function was sufficient to represent the anisotropy data to within the S/N level of the data. For the remaining solvents a second, faster component had to be added to the primary exponential component in order to achieve a satisfactory fit. In such cases sensible fits could usually be achieved by varying all four parameters, $r(0)$, a_1, τ_1, and τ_2, simultaneously. However, in the four most viscous solvents, components of the anisotropy decayed with time constants longer than 300 ps. Due to the limited scan range of the up-conversion instrument (1.1 ns), in these four solvents the time constant of the slower component (τ_2) was held fixed at the values determined from separate time-correlated single-photon-counting measurements.[74,75]

A summary of the fits to the anisotropy decay data is provided in Table 1. For the majority of the solvents, more than one data set was collected and averaged to obtain the final result listed. The column labeled "*N*" in this table indicates the number of independent measurements performed in a given solvent. Also listed under the heading "*Q*" is some indication of the overall quality anticipated for a given data set, with 1 indicating the highest and 3 the lowest quality results. (These assessments are based on overall S/N levels, the degree of the match between isotropic and magic decays, etc.) In cases where biexponential fit parameters are listed, the parameters are coupled such that individual values may not have particular significance. In these cases it is preferable to use as measures of the rotation times the initial time constant, τ_0,

$$\tau_0^{-1} = a_1/\tau_1 + (1 - a_1)/\tau_2 \quad (11)$$

and the average or correlation time $\langle\tau\rangle$,

$$\langle\tau\rangle = a_1\tau_1 + (1 - a_1)\tau_2 \quad (12)$$

which are also listed in Table 1. On the basis of the variations observed in repeated measurements, we expect the uncertainties ($2\sigma_m$) in these quantities to be on the order of $\pm 25\%/\sqrt{N}$ in τ_0 and $\pm 8\%/\sqrt{N}$ in $\langle\tau\rangle$.

Since observation of nonexponential anisotropy decays is relatively rare (especially in typical room temperature solvents), some further comment on the nonexponentiality observed with C153 is in order. First, we note that it is probably best to view the anisotropies of C153 in all solvents as being nonexponential functions of time. Different solvents can then be grouped into three classes according to the degree of departure from exponential behavior exhibited. As listed in Table 1, in roughly half of the solvents studied here the anisotropy is adequately represented by a single-exponential function of time. However, even in this first class of solvents a slight improvement in the pattern of residuals can be achieved by addition of a very small (<5%) fraction of a faster component. The second class of solvents is typified by the HMPA data shown in Figure 3. Here, although the amplitudes of the second component required to fit the data (∼10%) is rather small, the improvement in the fit when this second component is added is clearly significant. For example, in the HMPA data shown in Figure 3 the value of the χ_ν^2 statistic decreases from 2.1 to 1.0 upon addition of the second component. This nonexponentiality is nevertheless subtle and could easily be missed, especially in experiments where insufficient data are collected at early times. Finally, for the third class of solvents, which consists of many of the squalane mixtures and the normal alcohol solvents, the nonexponentiality in $r(t)$ is pronounced. An example of this type of behavior is provided by the 1-pentanol data shown in Figure 4. The obvious

TABLE 1: Summary of Solvent Properties and Rotational Anisotropy Decays[a]

solvent/solvation properties[c]						$r(t)$ data/fit parameters[d]						rotation times[e]		
solvent[b]	V_S (Å^3)	η (cP)	$\Delta\bar{\nu}$ (10^3 cm^{-1})	τ_ν (ps)	C_{el}	N	Q	$r(0)$	a_1	τ_1 (ps)	τ_2 (ps)	τ_0 (ps)	$\langle\tau\rangle$ (ps)	C_{obs}
n-hexane	113	0.29						0.369	1	13		13	13	0.46
hexanes	113	0.31				1	1	0.376	1	16		16	16	0.50
Sq/Hx 20%	137	0.54				1	1	0.373	1	21		2	21	0.39
nonane	164	0.67				2	1	0.373	1	29		29	29	0.44
cyclohexane	102	0.90				3	2	0.369	1	31		31	31	0.34
Sq/Hx 40%	171	1.05				1	1	0.377	0.37	11	58	22	40	0.39
Sq/Hx 50%	194	1.51				1	1	0.381	0.21	7.2	54	23	45	0.30
tridecane	232	1.71				2	2	0.367	1	60		60	60	0.35
Sq/Hx 60%	223	2.30				1	1	0.376	0.28	13	85	34	65	0.28
decalin	159	2.42				2	2	0.370	1	74		74	74	0.31
n-hexadecane	283	3.04						0.376	0.24	11	91	30	72	0.24
HMN	283	3.33						0.371	0.11	4.3	87	44	77	0.23
Sq/Hx 70%	262	3.68				2	1	0.369	0.19	14	94	44	78	0.21
Sq/Hx 80%	315	6.35				2	2	(0.374)	0.23	10	131	35	103	0.16
Sq/Hx 90%	394	12.4				1	2	0.376	0.24	17	192	54	150	0.12
squalane	521	28.3				1	2	0.369	0.24	30	(394)	98	304	0.11
acetone	65	0.30	1.80	0.58	0.090	1	1	0.380	1	19		19	19	0.64
acetonitrile	47	0.34	2.28	0.26	0.045	4	1	0.378	1	22		22	22	0.63
methyl acetate	71	0.36	1.43	0.85	0.088	2	1	0.376	1	23		23	23	0.63
dichloromethane	57	0.41	1.22	0.56	0.044	1	2	0.373	1	28		28	28	0.67
tetrahydrofuran	74	0.46	1.32	0.94	0.071	1	1	0.374	1	26		26	26	0.58
chloroform	71	0.54	0.81	2.8	0.11	4	1	0.373	1	42		42	42	0.78
toluene	98	0.55	0.93	2.7	0.12	1	2	0.376	1	29		29	29	0.53
DMC	77	0.59	1.80	1.4	0.11	1	1	0.372	1	35		35	35	0.60
benzene	80	0.60	0.83	2.0	0.074	3	1	0.377	0.08	2.7	32	16	29	0.49
nitromethane	51	0.61	1.84	0.40	0.032	1	2	0.373	1	36		37	36	0.60
dimethylformamide	78	0.80	1.98	0.92	0.059	2	1	0.373	1	47		47	47	0.59
hexafluorobenzene	108	0.86	0.95	3.7	0.11	1	1	0.376	0.12	3.0	56	18	50	0.58
1-butylbenzene	149	0.96	0.67	8.8	0.16	1	3	0.373	1	50		50	50	0.52
p-dioxane	80	1.20	1.26	1.7	0.046	2	2	0.380	0.05	3.7	61	34	59	0.49
benzonitrile	100	1.24	1.29	5.1	0.14	1	3	(0.374)	1	93		93	93	0.75
dimethyl sulfoxide	76	1.99	2.05	1.8	0.048	8	2	0.371	1	100		100	100	0.50
propylene carbonate	83	2.53	1.90	3.6	0.071	2	1	0.378	0.06	4.9	126	48	118	0.47
HMPA	183	3.10	1.49	9.5	0.12	5	1	0.366	0.129	9.7	158	53	139	0.45
methanol	36	0.55	2.34	5.0	0.56	5	1	0.375	0.231	5.9	44	17	35	0.64
ethanol	53	1.08	2.02	16	0.78	2	1	0.375	0.337	10.4	89	25	63	0.58
1-propanol	70	1.94	2.01	26	0.71	4	3	0.370	0.347	14.6	146	36	101	0.52
1-butanol	87	2.57	2.11	63	1.4	1	2	0.371	0.368	18.7	211	44	140	0.55
1-pentanol	104	3.51	1.92	103	1.5	4	2	0.378	0.446	32	(405)	65	238	0.68
1-decanol	189	11.0	2.07	260	1.3	1	2	0.375	0.366	110	(1220)	261	818	0.75
ethylene glycol	61	17.3	2.15	15	0.050	2	2	0.369	0.055	44	(880)	398	835	0.48
N-methylformamide	60	1.65	2.01	5.7	0.18	1	2	0.376	0.085	9.2	100	54	92	0.56
formamide	43	3.30	1.84	5.0	0.073	2	1	0.370	1.000	185		185	185	0.56
stick prediction		(1)							0.01	77	100	100	100	1
slip prediction		(1)							0.71	4.9	35	6.6	14	0.14

[a] Rotation and solvation data correspond to 22 ± 2 °C. [b] Solvents designated "Sq/Hx *X*%" indicate mixtures of squalane (2,6,10,15,19,23-hexamethyltetracosane) and hexanes with *X* the volume percentage of squalane. HMN denotes 2,2,4,4,6,8,8-heptamethylnonane, DMC is dimethyl carbonate, and HMPA is hexamethylphosphoramide. The rows labeled "stick" and "slip" are predictions based on the ellipsoid/hydrodynamic modeling discussed in section IVB. (Times are for a viscosity of 1 cP.) [c] van der Waals volumes (V_S) were calculated from the atomic increments tabulated in ref 76. Viscosities (η; 25 °C) of most solvents are from the compilations in ref 69, except for HMN, and the squalane mixtures, which were measured. $\Delta\bar{\nu}$ and τ_ν are characteristics of the time-dependent emission shift of C153. The magnitudes of the shift $\Delta\bar{\nu}$ are from ref 77 and the solvation times τ_ν are the average (as in eq 12) solvation times reported in refs 70 and 77. C_{el} is the ratio of the dielectric friction magnitude predicted from eq 7 to the magnitude of the friction predicted from stick hydrodynamics (eq 24). [d] N and Q denote the number of independent $r(t)$ determinations and an assessment of their overall quality (1 is best) in a given solvent. The values of $r(0)$, a_1, τ_1, and τ_2 are the average values (over N data sets) of the parameters of the biexponential fits of the $r(t)$ data according to eq 10. Cases in which the value of $r(0)$ is shown in parentheses indicate instances where this parameter was held fixed in the fitting. Values of τ_2 shown in parentheses are values determined from time-correlated single photon counting measurements.[74,75] (See text.) [e] τ_0 and $<\tau>$ refer to initial and average rotation times defined in eqs 11 and 12. Uncertainties ($2\sigma_m$) in these times are expected to be on the order of $\pm 25\%/\sqrt{N}$ in τ_0 and $\pm 8\%/\sqrt{N}$ in $\langle\tau\rangle$. C_{obs} denotes the observed value of the rotational coupling parameter defined by eq 3 (for $L = 2$).

nonlinearity displayed in this logarithmic plot signals the presence of (at least) two components of comparable amplitude and widely differing time constants in $r(t)$. Such highly nonexponential anisotropy decays were reported for C153 in several alcohols at reduced temperatures in our initial study on this probe.[72]

There are a number of possible explanations for nonexponential anisotropy decays. First, even within the context of hydrodynamic theories, nonexponential $r(t)$ functions can occur when the shape of the solute leads to very different friction on rotation about different axes. In the most general case, $r(t)$ for a nonspherical object undergoing diffusive rotation can decay with up to five time constants.[4,78] In section IVB we will discuss hydrodynamic models using an ellipsoidal shape to represent the C153 rotor. For now we simply use the results of such modeling, which are shown in Figure 4 and listed at the bottom of Table 1. As will be discussed later, the stick boundary condition is most realistic for modeling C153. For this case

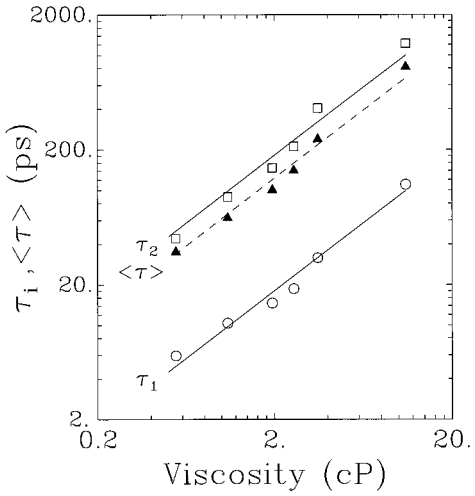

Figure 5. Time constants (open symbols) of biexponential fits to anisotropy decays of C153 in *n*-alcohols plotted as functions of solvent viscosity. Also shown (filled triangles) are the average or correlation times, $\langle\tau\rangle_{rot}$, determined from these fits via eq 12. The lines represent the proportionalities $\tau_1 = 9.0\eta$, $\tau_2 = 91\eta$, and $\langle\tau\rangle = 62\eta$.

the anisotropy decay is predicted to be indistinguishable from a single-exponential function of time. In addition, irrespective of the shape of the molecule and which boundary is applied, simple hydrodynamic theories would predict that the functional form of $r(t)$ should be independent of solvent, contrary to what is observed experimentally. Thus, simple hydrodynamic theories cannot explain the departure from exponential kinetics observed here.

A different explanation was offered in our early study of solvation dynamics using the C153 probe.[72] In that study, we noted a correlation between the time constant of the fast rotational component and the measured solvation time of C153 in several alcohol solvents. We conjectured that this faster rotational component might be directly connected to the solvation process in one of two ways. It could either reflect an actual rotational motion of the solute molecule driven by a misalignment of the reaction field after electronic excitation or, alternatively, it might reflect a rotation of the emission transition moment brought about by the dynamical solvation process. However, with the greater variety of solvents available in the present study, it is clear that neither of these explanations is tenable. When all of the polar solvents are considered together, one finds no direct correlation between τ_1 and the (average) solvation times. As in our earlier work, we do find a reasonable correlation between τ_1 and solvation times for the *n*-alcohol solvents. But this same correlation does not apply to other solvent types, as it should if one of these two general mechanisms were to apply. The observation of a correlation in the case of the *n*-alcohols is really only a secondary effect of the primary relationship between τ_1 and solvent viscosity. As illustrated in Figure 5, both τ_1 and τ_2 are highly correlated to solvent viscosity with the *n*-alcohol data set. It is only because solvation times are also correlated to viscosity within this homologous series that the two phenomena appear connected. In addition, Table 1 shows that a number of the nonpolar solvents studied here also show nonexponential $r(t)$ decays. Since in these latter cases negligible time-dependent solvation occurs,[70] the nonexponential behavior observed here cannot be directly caused by the solvation process.

So then, what is the source of the nonexponentiality in $r(t)$? We believe the most likely explanation is that the nonexponential decays observed here reflect a departure from the strict Markovian limit of rotational motion. That is, at least in some solvents, the rotation of C153 is rapid enough that it senses more than just the time-integrated friction of the solvent; i.e., it is sensitive to the actual time dependence of the friction. In the limit where inertial solute dynamics can be neglected, the relation between the rotational correlation function $C_{rot}(t) = r(t)/r(0)$ and the time-dependent friction $\zeta(t)$ can be expressed by[79]

$$\tilde{C}_{rot}(s) \equiv \int_0^\infty e^{-st} C_{rot}(t)\, dt = \left\{ s + \frac{6kT}{\tilde{\zeta}(s)} \right\}^{-1} \qquad (13)$$

where $\tilde{\zeta}(s)$ (like $\tilde{C}_{rot}(s)$) represents the Laplace transform of the time-dependent friction function. If the solvent fluctuations responsible for $\zeta(t)$ decay much more rapidly than the solute rotates, one can approximate $\tilde{\zeta}(s) \cong \tilde{\zeta}(0) \equiv \zeta$, and $C_{rot}(t)$ is then an exponential function of time with time constant $\tau_{rot} = \zeta/6k_BT$. However, if $\zeta(t)$ contains components which decay on a time scale that is not rapid compared to the solute rotation, $C_{rot}(t)$ is not a simple exponential function of time. We propose that this is in fact true in many of the solvents studied here.

To examine whether this idea seems reasonable, we can ask what would be required of the time-dependent friction in order to produce the sorts of $C_{rot}(t)$ (or $r(t)$) decays observed. On the basis of molecular dynamics simulations of small-molecule solvents,[5,80] one anticipates $\zeta(t)$ should be bimodal, consisting of some subpicosecond component, related to the inertial characteristics of solvent molecules, along with much slower components related to diffusive solvent motions. The simplest model for $\zeta(t)$ is therefore a biexponential function of the form[81]

$$\frac{\zeta(t)}{\zeta(t=0)} = (1-f)e^{-t/\tau_1} + fe^{-t/\tau_2} \qquad (14)$$

where τ_1 and τ_2 correspond to the fast and slow components, respectively. The time-zero amplitude is set by the observed rotational correlation time, $\langle\tau\rangle_{rot} \equiv \int_0^\infty C_{rot}(t)\, dt = C_{rot}(0)$, via the relation

$$\frac{\zeta(t=0)}{6kT} = \frac{\langle\tau\rangle_{rot}}{(1-f)\tau_1 + f\tau_2} \qquad (15)$$

Model calculations with this functional form show that, for τ_1 less than $\langle\tau\rangle_{rot}/100$, the nonexponentiality of $C_{rot}(t)$ should become noticeable at our S/N levels when the fraction of the slow component (f) is greater than ~10% and when its time constant (τ_2) is simultaneously greater than $\langle\tau\rangle_{rot}/5$. We do not know the complete time dependence of $\zeta(t)$ in the solvents examined here. However, for the polar solvents, solvation dynamics measurements provide a characterization of at least that part of $\zeta(t)$ which arises from long-range electrostatic interactions (i.e., the dielectric friction part). We observe that there is a one-to-one correspondence between those polar solvents whose rotational anisotropies are clearly nonexponential (which we take to be those with $a_1 > 10\%$ in Table 1) and those whose solvation response functions ($S_\nu(t)$, tabulated in refs 70 and 77) show substantial (>10%) components with time constants greater than $\langle\tau\rangle_{rot}/5$. This correspondence strongly suggests that we are indeed observing the effects of non-Markovian friction on the rotational motion and that furthermore the time dependence of $\zeta(t)$ is at least loosely connected with the time dependence of electrostatic solvation.

We can proceed somewhat further in this analysis by attempting to directly fit the $r(t)$ using a biexponential $\zeta(t)$ model. Results of several such fits are compared to solvation dynamics data in Table 2. Since the actual $\zeta(t)$ functions are probably more complicated functions of time, the fitting parameters so obtained should be viewed as providing only a

TABLE 2: Rotational Friction and Solvation Response Functions

		rotational friction, $\zeta(t)$[b]					solvation dynamics, $S_v(t)$[c]				
solvent[a]	$\langle\tau\rangle_{rot}$ (ps)	$\zeta(t=0)$ (ps)	τ_1 (ps)	f (%)	% ζ	τ_2 (ps)	a_n (%)	τ_n (ps)	a_{n-1} (%)	τ_{n-1} (ps)	a(<1 ps) (%)
squalane	304	94	.98	1.9	69	112					
benzene	29	65	.30	2.9	37	5.9	3	25	60	1.9	37
hexafluorobenzene	50	65	.34	4.1	57	11	58	6.2			42
propylene carbonate	118	104	.54	4.1	54	15	22	6.6	24	2.0	55
HMPA	139	147	.39	1.8	59	30	23	30	40	7.2	37
methanol	35	108	.20	0.8	40	17	26	15	30	3.2	44
ethanol	63	99	.27	0.8	58	46	50	30	18	5.0	32
1-propanol	101	9.1	3.2	10.	68	59	52	48	23	6.6	25
1-butanol	140	38	1.1	2.8	70	92	34	133	39	43	16
1-pentanol	238	140	.45	0.7	71	168	65	151	25	22	11

[a] Solvents and average rotation times $\langle\tau\rangle_{rot}$ as listed in Table 1. [b] Parameters characterizing the time-dependent friction ζ(t) deduced from fitting anisotropy data ($C_{rot}(t)$; eq13) to a biexponential function, eq 14. [c] Characteristics of the solvation response functions (S_v(t)) measured from the time-resolved emission shifts of C153.[70] "a_n" and "a_{n-1}" denote the amplitudes and "τ_n" and "τ_{n-1}" the time constants of the two longest components in a multiexponential representation of $S_v(t)$. "a(<1 ps)" is the total amplitude of all components with time constants less than 1 ps.

qualitative description of $\zeta(t)$. They do, however, illustrate several interesting points. First, in most cases examined here a single-exponential representation of $\zeta(t)$ does not yield acceptable fits to the anistropy data. Fits using a biexponential representation, as listed in Table 2, are sufficient to fit the observed $r(t)$ decays to within the S/N of the experimental data. In all cases studied the $\zeta(t)$ functions obtained from biexponential fits were found to consist of a dominant fast component (usually $(1 - f) > 90\%$) having a subpicosecond time constant, together with a much slower and more variable component having an amplitude (f) of only a few percent. These features are in general agreement with the expected behavior of $\zeta(t)$ mentioned above. In addition, the longer of the two time constants determined from such fits is remarkably similar to the longest component of the solvation response of the various solvents, which are listed in the column labeled "τ_n" in Table 2. This is especially true in the normal alcohol solvent series. Thus, it again appears that the measured solvation response functions provide some indication of the time scales involved in $\zeta(t)$. However, we note that the *amplitudes* of the fast and slow components of the solvation response and of the rotational friction are quite different. Thus, while the amplitudes of the slowest solvation components ("a_n") typically account for over 25% of the solvation response in these solvents, they often represent less than 5% of $\zeta(t)$. (It is important to note that in spite of this small amplitude in $\zeta(t)$ the relative contribution of the slow component to the integrated rotational friction constant is large since it is the product $f\tau$, listed as "% ζ" in Table 2, that determines the rotational friction constant, not the amplitude itself.)

B. Rotation Times in Polar and Nonpolar Solvents: Dielectric Friction? We now dispense with further discussion of the detailed time dependence of $r(t)$ and henceforth focus on the average rotation times $\langle\tau\rangle_{rot}$ determined using eq 12. In cases when $r(t)$ is not a single-exponential function of time, it is this average or correlation time which is directly related to the total or integral friction constant ζ by

$$\langle\tau\rangle_{rot} \equiv \int_0^\infty C_{rot}(t)\,dt = \frac{\zeta}{6k_BT} \equiv \frac{1}{6k_BT}\int_0^\infty \zeta(t)\,dt \quad (16)$$

In Figure 6 we explore the relationship between these average rotation times and solvent viscosity. In this and the following figures, solvents have been divided into three categories: nonpolar, polar aprotic, and hydrogen-bond-donating solvents. Nonpolar solvents include only hydrocarbons, whereas the polar aprotic class includes several nondipolar but nevertheless polar[77] solvents such as benzene and dioxane.

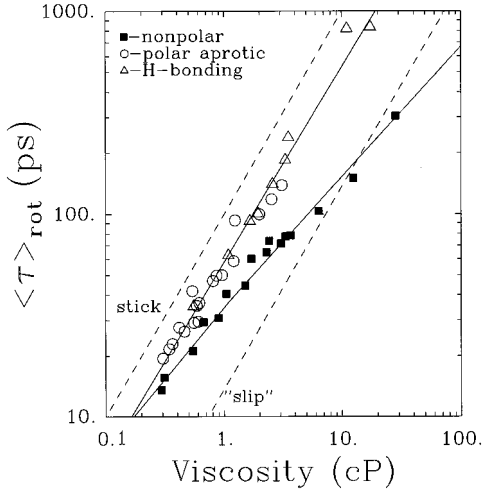

Figure 6. Average rotation times (or rotational correlation times) plotted versus solvent viscosity. Filled squares correspond to nonpolar (alkane) solvents, circles are polar aprotic solvents, and triangles are hydrogen-bond-donating solvents. (See Table 1 for a listing of the solvents included in each class.) The solid lines through these data are the logarithmic fits described in the text. The dashed lines are the average rotation times predicted from hydrodynamic calculations assuming an ellipsoidal shape and slip and stick boundary conditions. (See text for details.)

The most striking feature of Figure 6 is that nonpolar solvents follow a different correlation with viscosity than the remaining solvents. From logarithmic fits of the data one finds

$$\text{nonpolar:}\quad \langle\tau\rangle_{rot} = (34.8 \pm 4.1)\eta^{0.63\pm0.02} \qquad (N = 16,\ R = 0.98)$$

$$\text{polar + H-bonding:}\quad \langle\tau\rangle_{rot} = (58.1 \pm 1.6)\eta^{0.96\pm0.03} \qquad (N = 27,\ R = 0.99)$$

(These fits are for $\langle\tau\rangle_{rot}$ in picoseconds and η in centipoise. Uncertainties are ±1 standard deviation, and N and R are the number of data points and the correlation coefficient of the double-logarithmic fit.) There is no significant difference observed between the behavior of polar aprotic and hydrogen-bonding solvents. A similar lack of sensitivity to hydrogen bonding was previously observed with respect to solvation shifts of this molecule.[70,77] The polar + hydrogen-bonding solvents behave much as would be expected from a purely hydrodynamic model. That is, to a reasonable first approximation the average rotation times are proportional to viscosity and independent of solvent. Linear fits of $\langle\tau\rangle_{rot}$ vs η for all such solvents with viscosities less than 3 cP yield equally good fits either with or

without the inclusion of a small nonzero intercept. In contrast, the alkane solvents show a "nonhydrodynamic" power-law dependence on viscosity. Attempts to fit the lower viscosity data ($\eta \leq 3$ cP) to a linear function of viscosity yield unrealistically large $\eta = 0$ intercepts ($\langle\tau\rangle_{rot} = 11.2 + 23.2\eta$; $N = 11$, $R = 0.97$). Similar power-law behavior has been observed in a number of other cases previously.[82,83] As we will discuss shortly, this deviation from hydrodynamic behavior is probably best understood in terms of the presence of some factor in addition to solvent viscosity that makes the solvent−solute coupling (C) vary with solvent.

We have also included in Figure 6 the results of hydrodynamic calculations for ellipsoids using both stick and slip boundary conditions. These predictions were made as follows. Based on van der Waals increments,[76] the molecular volume of C153 is 246 Å^3. Using molecular modeling software, we find that shape of C153 can be reasonably approximated by an ellipsoid with semiaxis dimensions $a = 2.0$, $b = 4.8$, and $c = 6.1$ Å. (These values were arrived at by choosing the c semiaxis length to be half of the largest dimension of C153, the shortest semiaxis to represent the thickness of the aromatic plane, and the intermediate axis to reproduce the total volume of the molecule.) Semiempirical calculations[84] place the $S_0 \leftrightarrow S_1$ transition moment approximately parallel to the longest axis of the ellipsoid. Using this representation of the molecular shape and transition moment direction, time-dependent anisotropies were calculated as described in ref 4 using friction coefficients calculated from Perrin's equations for the f factor[10] and the C factor appropriate for slip boundary conditions obtained by interpolating the numerical tabulations of Youngren and Acrivos.[15] The $r(t)$ functions so obtained are biexponential functions of time whose components are listed at the bottom of Table 1. (See also Figure 4.) In Figure 6 we have plotted the average times associated with these $r(t)$ functions, which are strictly proportional to solvent viscosity. As can be seen in this figure, nearly all of the experimental data lie between the rather broad limits set by these two hydrodynamic calculations. The polar solvent data lie closer to the stick predictions but are faster than the stick line by roughly a factor of 2. The alkane data are generally closer to the slip predictions and appear to be going subslip at the highest viscosities. However, some discretion must be applied when comparing the experimental data to these ellipsoid-based slip calculations. Whereas the stick predictions are likely to be an accurate approximation to the results that would be obtained from a hydrodynamic calculation using the true shape of the molecule, the slip calculations probably are not. The reason is that, for an ellipsoid of the shape defined above, the friction constant for the spinning motion of the molecular plane, which contributes the dominant part of $r(t)$, is a strong function of the aspect ratio c/b. (This is not true in the stick case.) Under the slip boundary condition only motions that displace solvent give rise to any friction. For the nearly-oblate ($b \cong c$) shape chosen to represent C153 here, the amount of solvent displacement required for this spinning motion is probably significantly underestimated. The rapid rotation (and the degree of nonexponentiality in $r(t)$) is therefore probably exaggerated by use of the ellipsoidal model and should only be a rough approximation to the complete slip prediction which would be obtained using the real molecular shape. (We are currently investigating the use of all-atom models[85] to obtain better approximations to the true slip-limit friction constants.)

We now consider what might give rise to the rather remarkable difference in rotation times shown by polar and nonpolar solvents of the same viscosity. A natural interpretation of Figure 6 would be that the large dipole moment of C153 (∼15 D in S_1[86]) results in stronger coupling to polar solvents than to nonpolar solvents of the same viscosity, i.e., that an extra, "dielectric" friction operates so as to slow the rotation of C153 in polar solvents. As discussed in section II, one can distinguish two limiting cases wherein such effects are ascribed either to specific interactions (solvent attachment) or to nonspecific electrostatic forces. Since the first of these possibilities has been discussed recently in conjunction with a molecule nearly identical to C153, we discuss this possibility first.

In a recent study Moog *et al.*[75] observed that coumarin 102 (the analogue of C153 in which the CF_3 group is replaced by CH_3 group) rotates more slowly in bulk alcohol solvents than in alkanes. They also showed that when diluted in alkane solvents, 1:1 complexes form between C102 and alcohols such as trifluoroethanol (TFE). The rotation times measured in such solutions could be understood in terms of long-lived solute−alcohol complexes rotating as a whole. (The C═O site, which is both highly charged and solvent accessible, was assumed to be the likely site of hydrogen bonding with alcohols.) They noted that the difference between the rotation times of C102 in neat TFE and in an isoviscous alkane solvent could be rationalized equally well either by assuming that similar complexes are present in the bulk alcohol solvent or by the operation of nonspecific dielectric friction effects. For reasons of simplicity Moog et al. preferred the former picture. Since C153 is similar to C102 in size, shape, and electronic charge distribution, one would expect nearly identical rotation times and hydrogen-bonding behavior for the two solutes. Indeed, the rotation times of C102 in TFE and in decalin studied in ref 75 fit nicely on the C153 correlations shown in Figure 6. But, with the additional data available in the present study, it now appears that solvent attachment *cannot* explain why the rotation times of C153 differ in isoviscous alkane and bulk alcohol solvents. If solvent attachment were a critical factor, one would expect to observe a clear distinction between polar solvents that can and cannot form specific complexes with C153, contrary to what is observed here.

It is worth pausing to comment on this lack of distinction between hydrogen-bonding and polar aprotic solvents. Both chemical intuition and computer simulations[87] indicate that in bulk alcohol solvents there is nearly always at least one hydrogen bond made between a solvent molecule and the C═O site of C153. Why then does the presence of this relatively strong hydrogen bond not lead to a different rotation time−viscosity correlation in such solvents compared to other polar solvents? That is, why does C153 not appear "bigger" in bulk alcohol solvents in the same way that C102 in dilute TFE solutions appears bigger due to the attachment of a single TFE molecule? There are two possible explanations. First, whether such a solventberg perspective is appropriate in bulk solution depends on the longevity of complexes relative to the rotation time. In bulk alcohol solvents (especially in shorter *n*-alcohols) solvent molecules would be expected to exchange on a much faster time scale than in dilute solution. Second, it may well be that hydrogen bonding between the solute and solvent is actually a *necessary* condition for observing comparable rotational behavior in alcohols and non-hydrogen-bonding solvents. The large viscosities of hydroxylic solvents when compared to aprotic solvents arise mainly due to the presence of hydrogen bonding between solvent molecules. If there were *no* solvent−solute hydrogen bonds present, one might expect the friction experienced by the rotating solute would be *less than* that indicated by the bulk solvent viscosity. In fact, just this sort of behavior is observed for polyaromatic hydrocarbon solutes

rotating in alcohol solvents.[20] In such systems the rotation times are usually found to be subslip, i.e., much less than what is expected based on the solvent viscosity. We therefore conjecture that *the comparable rotational behavior exhibited by C153 (and probably also C102) in protic and polar aprotic solvents reflects a similarity in the hydrogen-bonding statics/dynamics between the solute and solvent and between molecules in the neat solvent itself.*

Having considered specific solvation effects, we now ask whether nonspecific dielectric friction effects can explain the differences between polar (both protic and aprotic) and nonpolar (alkane) solvents. To do so, we will first assume that the difference in rotation times between a polar solvent and an isoviscous nonpolar solvent is a direct measure of the dielectric friction effect. Using the correlation established for the rotation times of alkane solvents (τ_{np}), we can thus test the differences,

$$\langle\tau\rangle_{rot} - \tau_{np}(\eta) = \langle\tau\rangle_{rot} - 34.8\eta^{0.63} \qquad (17)$$

for proportionality to the dielectric component of the friction, ζ_{el} in eq 4. The least model-dependent measure of the magnitude of the dielectric friction expected in a given solvent is provided by the van der Zwan−Hynes connection (eq 7). This relation states that ζ_{el} should be proportional to the product $(\Delta\bar{\nu}\langle\tau\rangle_\nu)$, where $\Delta\bar{\nu}$ is the magnitude and $\langle\tau\rangle_\nu$ the average time constant of the solvation shift observed in a given solvent. Thus, if the separation between polar and nonpolar solvents in Figure 6 is indeed a manifestation of nonspecific dielectric friction, we should observe the relation

$$\langle\tau\rangle_{rot} - \tau_{np}(\eta) = A(\Delta\bar{\nu}\tau_\nu)_{solv} \qquad (18)$$

with A being a solvent-independent proportionality constant. In the case where a point dipole representation of the solute's charge distribution is valid, this constant should be given by

$$A = \frac{hc}{6k_BT}\frac{\mu_e^2}{(\Delta\mu)^2} \qquad (19)$$

where μ_e is the excited-state dipole moment and $\Delta\mu$ the change $(S_1 - S_0)$ in dipole moment of the solute.

Figure 7 shows the comparison between $\langle\tau\rangle_{rot} - \tau_{np}$ and $(\Delta\bar{\nu}\tau_\nu)_{solv}$. The solvation shifts and times used in this comparison are from the previous studies of time-resolved emission shifts of C153 reported in refs 70 and 77. (For convenience, the relevant quantities are also reproduced in Table 1.) The solid line in Figure 7 represents use of the proportionality constant $A = 2.63 \times 10^{-3}$ cm calculated assuming a point dipole solute and values $\mu_e = 15$ D and $\Delta\mu = 8.3$ D.[77,86,88] The correlation between the rotation time difference and the predicted dielectric friction is relatively poor when all solvents are considered together. (A linear fit of these log−log data yields a correlation coefficient of $R = 0.83$ with 27 data points.) In part, this poor fit is due to the fact that the normal alcohols exhibit a different correlation from the polar aprotic solvents and from other hydrogen-bonding solvents. Whereas the observed difference $\langle\tau\rangle_{rot} - \tau_{np}$ is generally larger than the dielectric friction estimate (solid line) in other solvents, in the normal alcohols the observed difference is about 3-fold smaller than predicted. In addition, we note that within just the normal alcohol series, the correlation between $\langle\tau\rangle_{rot} - \tau_{np}$ and $(\Delta\bar{\nu}\tau_\nu)_{solv}$ is rather good. However, this correlation in the *n*-alcohols, and indeed any overall correlation observed in Figure 7, is largely fortuitous. Rather than there being a direct causal relationship between the observed $\langle\tau\rangle_{rot} - \tau_{np}$ and $(\Delta\bar{\nu}\tau_\nu)_{solv}$, the correlation between these variables in Figure 7 is in fact better understood as being a secondary result of the strong correlation that exists between $\langle\tau\rangle_{rot} - \tau_{np}$ and solvent viscosity. As could be anticipated from the data in Figure 6, a plot of $\langle\tau\rangle_{rot} - \tau_{np}$ versus solvent viscosity yields a much higher degree of correlation ($R = 0.97$) than what is shown in Figure 7. Furthermore, the normal alcohols no longer appear distinct from the other solvents in such a plot. Thus, what correlation is observed between $\langle\tau\rangle_{rot} - \tau_{np}$ and $(\Delta\bar{\nu}\tau_\nu)_{solv}$ in Figure 7 mainly reflects the fact that solvation times, which are primarily responsible for variations in the product $(\Delta\bar{\nu}\tau_\nu)_{solv}$, are at least roughly correlated to solvent viscosity. The correlation between τ_ν and solvent viscosity is rather good when one stays within a homologous family of solvents such as the *n*-alcohols, thus the much better correlation with this selected set of data in Figure 7 is understandable.

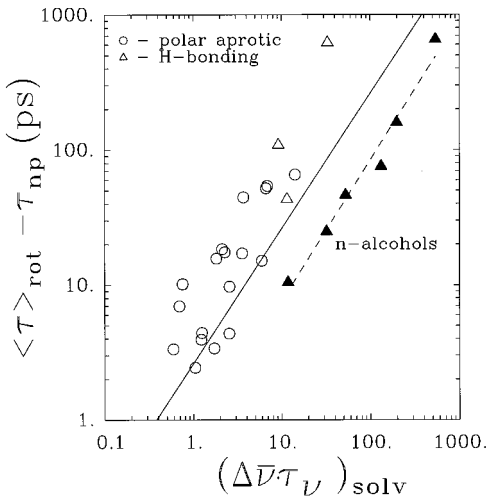

Figure 7. Comparison of "excess rotation times" in polar solvents, $\langle\tau\rangle_{rot} - \tau_{np}(\eta)$, to the solvation product $\Delta\bar{\nu}\tau_\nu$ (in units of 10^3 cm^{-1} ps). The latter product is predicted to be proportional to the magnitude of the dielectric friction according to the van der Zwan and Hynes connection (eqs 7 and 18). Circles denote polar aprotic solvents and triangles hydrogen-bonding solvents. The solid line represents the complete prediction of eq 18 using the proportionality constant $A = 2.63 \times 10^{-3}$ cm, determined from the dipole solute approximation as described in the text. Data in normal alcohol solvents are plotted as filled symbols to show their distinction from all of the remaining solvents. The dashed line through these alcohol points shows a fit with the proportionality constant $A = 0.68 \times 10^{-3}$ cm.

Based on the above results, it does not appear that the large differences between rotation times of C153 in polar and isoviscous nonpolar solvents can be directly attributed to dielectric friction. As we will show presently, there are other effects that are at least as important in determining these differences in the case of C153. But before closing this section, it is useful to point out a lesson that Figure 7 provides. We note that many past studies of dielectric friction have concentrated attention on only one or perhaps two series of solvents, and in most cases the *n*-alcohols were one of the series selected (because dielectric friction is predicted to be greatest in these solvents). The considerations just discussed with respect to Figure 7 indicate that caution should be used when drawing conclusions about trends observed with such limited data sets. Since many factors vary systematically along a solvent series such as the *n*-alkohols (i.e., viscosity and solvation time in the present case), it is often not possible to cleanly associate observed variations with only the particular variable one has in mind.

C. Effect of Solvent Size. If dielectric friction is not the primary source of the remarkable difference between the rotation times of C153 in polar and nonpolar solvents, what is? A clue is provided by the nonlinear dependence of $\langle\tau\rangle_{rot}$ on η in

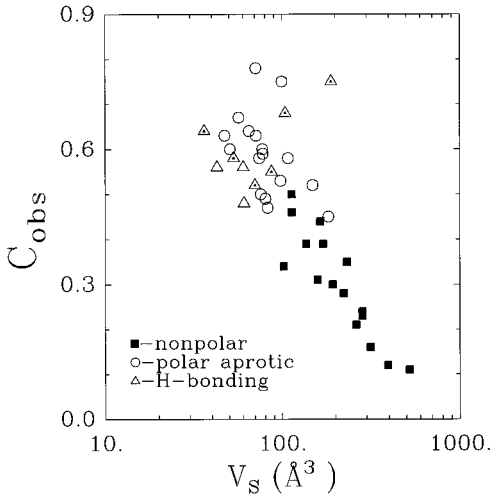

Figure 8. Observed rotational coupling parameters $C_{obs} \equiv \langle\tau\rangle/\tau_{stick}$ (eq 3) versus the van der Waals volume of solvent molecules, V_S. A value of $\tau_{stick} = 99.8\eta$ was used for calculation of C_{obs}.

nonpolar solvents. As Zwanzig and Harrison[13] point out, there are fundamental reasons why friction should be proportional to the first power of solvent viscosity. They therefore argue that any other type of dependence is best viewed as reflecting a change in the coupling parameter with some other solvent property that simultaneously varies along with its viscosity. We therefore switch attention from the rotation times themselves to the observed values of the rotational coupling parameters defined here by

$$C_{obs} = \langle\tau\rangle_{rot}/\tau_{stick} \tag{20}$$

Viewing these ratios removes the "correct" viscosity dependence (through the use of τ_{stick}) and better enables one to discern what other solvent features might be giving rise to the unexpected viscosity behavior. (We use τ_{stick} in preference to η itself for this purpose since the former value provides an exact benchmark ($C = 1$) that should be approached in the limit of vanishing solvent size.)

While there is no single solvent property that completely accounts for the solvent variation of C_{obs}, one property that is well correlated to this coupling parameter is the size of solvent molecules. In Figure 8 we illustrate this point using the van der Waals volume of the solvent (V_s) as the size measure. Despite the presence of a large amount of scatter in the data, there is a clear trend of decreasing coupling parameter with increasing solvent size, especially among the nonpolar solvents. We note that such behavior is not unique to C153. A number of past studies on a variety of solutes have reported a nonlinear viscosity dependence of rotation times[82,83] and/or a variation in C_{obs} with solvent size similar to those observed here.[46,89−93] (Unlike the present work, nearly all past studies had examined nonpolar solutes in a series of *n*-alkane solvents.) For our purposes, a critical observation to be made from Figure 8 is that, when the data are plotted in this manner, there is no longer an obvious distinction between the behavior of nonpolar and polar solvents. The main difference between these two classes of solvents appears to be that, in order to obtain comparable viscosities, the nonpolar solvents are substantially larger then their polar counterparts. Thus, rather than being due to dielectric friction effects, at least a large part of the difference in rotation times of C153 in polar versus nonpolar solvents can be attributed to this size effect on the coupling coefficient. If there is also a dielectric friction effect, in order to use comparisons between polar and nonpolar solvents to detect it, one must first be able to understand or at least empirically model the size dependence.

A dependence of the solute−solvent coupling on solvent size, while not predicted by purely hydrodynamic theories, should be expected from a molecular perspective. Both the strength and the time scale of the solute−solvent interactions which determine the friction should partially depend on the relative sizes of solute and solvent molecules. There are two theories that can be readily applied to model this size effect. The first is the relatively old theory proposed by Geirer and Wirtz in 1953.[24] These authors envisioned the solute to be surrounded by concentric shells of solvent, each a solvent molecule diameter in thickness. By considering how the angular velocity of solvent molecules surrounding the rotating solute should decrease as function of distance away from the solute, Geirer and Wirtz derived the following expression for *C*:

$$C_{GW} = (1/6\rho)S^{-1} \tag{21a}$$

where

$$S \equiv \sum_{m=0}^{\infty}(1 + 2m\rho)^{-4} \tag{21b}$$

and $\rho \equiv V_S/V_P$ is the ratio of solvent ("S") to solute ("P" = probe) volumes. There are no adjustable parameters in this theory, perhaps with the exception of how one chooses to define the solute and solvent volumes. (Here we will consistently employ van der Waals volumes.)

The second theory we consider is from the more recent work of Dote, Kivelson, and Schwartz (DKS[25]). In this theory the solvent−solute coupling is viewed as being a function of the ratio of its size to the free volume (ΔV) available to the rotating solute. Their result for *C* can be written

$$C_{DKS} = (1 + \gamma/\phi)^{-1} \tag{22a}$$

with

$$\gamma = (\Delta V/V_S)\rho(4\rho^{-2/3} + 1) \tag{22b}$$

The factor γ/ϕ is the ratio of the free space available to the solute (γV_P) to its effective rotational volume (ϕV_P). The parameter ϕ is taken to be the ratio of the rotation time predicted by slip hydrodynamics to the stick prediction for the sphere of the same volume. For C153, this value is 0.28. The one input to the DKS theory that is hard to determine unambiguously is the free volume of the solvent. Free volume is a theoretical construct that can only be determined from semiphenomenological theories for properties such as viscosity and diffusion constants.[94] For this quantity, we use the free volumes *of* n-alkanes determined from viscosity data by Ben-Amotz and Drake.[89] In order to simplify the calculations and their interpretation, we parametrize these free volumes using the approximate proportionality: $\Delta V/V_S \simeq 0.334$. By virtue of this choice, C_{DKS}, like C_{GW}, varies with solvent only through the solvent−solute size ratio ρ.

Figure 9 illustrates the predictions of these two theories in the form of a plot of $(1/C - 1)$ versus ρ. This particular format is suggested by the fact that both theories predict that the coupling parameter should approach unity (i.e., the stick limit) as $\rho \rightarrow 0$ and that $1/C$ should be proportional to some increasing function of ρ as $\rho \rightarrow \infty$. Figure 9 shows that, over the range of values of ρ typical in experiment, both theories predict an approximate power-law dependence on this size ratio, $(1/C - 1) \propto \rho^{\alpha}$, with $\alpha_{GW} \sim 1$ and $\alpha_{DKS} \sim 1/3$.

The experimental data shown in Figure 9 are also consistent with this type of power-law relationship. To demonstrate that

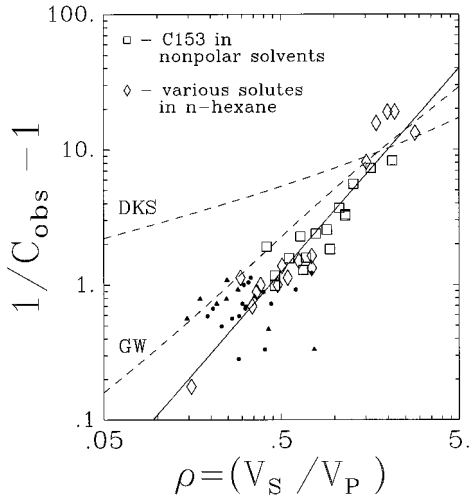

Figure 9. Rotational coupling parameters (plotted as $1/C_{obs} - 1$) versus the solvent/solute size ratio ρ. Large squares denote data for C153 in nonpolar solvents. Data for C153 in polar solvents are also shown as small filled symbols. The large diamonds denote values calculated for the collection of assorted solutes in *n*-hexane compiled in ref 89. The solid line is the fit (eq 23) to all of the nonpolar solvent data (open symbols). The dashed curves are the predictions of the Geirer−Wirtz[24] and Dote-Kivelson−Schwartz[25] theories.

such behavior is relatively general, in addition to the C153 data (open squares), we have also plotted a second set of data (diamonds) previously compiled by Ben-Amotz and Drake.[89] These authors collected and compared the rotation times of a series of 16 solutes ranging in size from OCS ($V_P = 40$ Å^3) to the large molecule "BTBP" (733 Å^3) all in a single reference solvent, *n*-hexane. As can be seen from Figure 9, both sets of data appear to follow the same correlation with ρ. Fitting all of these data simultaneously yields the approximate relation:

$$1/C_{obs} - 1 = (3.53 \pm 0.24)\rho^{1.51\pm0.09} \quad (N = 32, R = 0.94) \tag{23}$$

Comparing this empirical correlation with the theoretical predictions, we find that the Geirer−Wirtz theory is in reasonable accord with experiment. For a typical value of $\rho = {}^1/_2$ this theory predicts $C_{GW} = 0.31$, compared to the observed value $C_{obs} \sim 0.44$. Furthermore, the dependence on the solvent/solute size ratio is only slightly underestimated by the Geirer−Wirtz theory. In contrast, the DKS theory does a poor job of modeling the present data. For $\rho = {}^1/_2$ the predicted value of $C_{DKS} = 0.16$, a factor of 3 smaller than experiment. More importantly, the dependence on ρ predicted by the DKS theory is much weaker than observed in the experimental data.[95]

D. Dielectric Friction Revisited. The coupling factors observed for C153 in polar solvents, shown as small filled symbols in Figure 9, are roughly consistent with the correlation observed in nonpolar solvents. The main difference appears to be a larger degree of scatter among the polar data, undoubtedly the result of the much greater variety of solute−solvent interactions present with this set of solvents. As already noted, in the solvents studied here the average value of ρ is significantly smaller for the polar solvent set, and as anticipated from the nonpolar solvent correlation, the values of C_{obs} are on average larger for these solvents. This size difference can account for the majority of the differences observed between the rotation times in polar and nonpolar solvents, without invoking dielectric friction effects. However, we now use what we have learned about size effects from the nonpolar solvents and examine whether dielectric friction might be able to at least account for the scatter observed in the polar data in Figure 9.

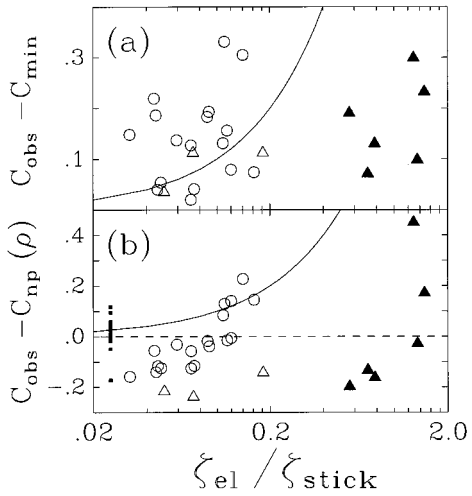

Figure 10. Comparison of the "residual coupling parameters" in polar solvents to the predicted dielectric friction contribution to the rotational coupling (eq 24). The residual coupling is defined as C_{obs} minus the contribution to the solvent−solute coupling due to "hydrodynamic" interactions. The latter quantity is estimated in two ways. In (a) it is assume that C_{hyd} is approximately the same for all polar solvents. For purposes of presentation we have subtracted off the minimum value observed in the polar solvent set ($C_{min} = 0.45$ in HMPA). In (b) C_{hyd} is estimated using the ρ dependence described by eq 23. Circles denote polar aprotic solvents, and triangles denote hydrogen-bonding solvents. Normal alcohols are shown as filled triangles. In (b) we also show points corresponding to $C_{obs} - C_{np}(\rho)$ for the nonpolar solvents (small filled squares) in order to illustrate the scatter about eq 23 in these solvents. (The latter data are plotted at an arbitrary value of ζ_{el}/ζ_{stick}.) The solid curves on both panels indicate equality between the ordinate and abscissa values.

In Figure 10 we therefore reconsider the possible role of dielectric friction, this time focusing on the coupling parameters rather then the rotation times. To do so, we will use an estimate of the dielectric friction effect on the overall coupling constant,

$$C_{el} \equiv \zeta_{el}/\zeta_{stick} \tag{24}$$

with ζ_{el} calculated using observed solvation data and the van der Zwan−Hynes connection, eq 7. (The values of C_{el} so calculated are provided in Table 1.) Given the basic assumption of the separability of dielectric and other sources of friction (eq 4), one expects that the observed coupling parameter can be decomposed as

$$C_{obs} = C_{hyd} + C_{el} \tag{25}$$

In Figure 10 we have employed two methods for estimating the "hydrodynamic" part of the coupling parameter, C_{hyd}. In (a), we assume that to a first approximation the hydrodynamic coupling is the same for all polar solvents. For the sake of presentation we further assume that this uniform value of C_{hyd} is given by the minimum value of C_{obs} within the polar solvent set ($C_{min} = 0.45$, which occurs in HMPA). We thus compare $C_{obs} - C_{min}$ to ζ_{el}/ζ_{stick}. In (b) we instead assume that the hydrodynamic part of C_{obs} follows the same correlation with solvent size in polar solvents as it does in nonpolar solvents. In this panel we therefore compare $C_{obs} - C_{np}(\rho)$ to ζ_{el}/ζ_{stick}, where $C_{np}(\rho)$ is the value of C_{hyd} calculated using eq 23.

Figure 10 shows that there is relatively little correlation between the "extra" solute−solvent coupling and the expected dielectric friction in polar solvents. The curved lines in both panels represent equality between the values of C_{el} determined from the rotation times and the friction ratio ζ_{el}/ζ_{stick}. Note that for ease of comparison we have calculated ζ_{el} explicitly from

eq 7, including the factor of $\mu_e^2/(\Delta\mu)^2$. Although this proportionality constant is strictly correct only for a point dipole solute, alteration of this factor would only shift the points along the logarithmic horizontal axis and would therefore lead to no better agreement between C_{el} and ζ_{el}/ζ_{stick}. As previously seen in Figure 7, there is a clear distinction between the normal alcohols (filled triangles) and the remaining solvents. The majority of the solvents, mainly the polar aprotics, are clustered around relatively small values of ζ_{el}/ζ_{stick}. If no account is made of solvent size effects (panel a), the observed coupling parameters in these solvents show no correlation at all to the predicted dielectric friction contributions. If the size dependence is taken into account (panel b), some hint of a correlation may be found, especially in the polar aprotic solvents. However, using $C_{np}(\rho)$ to determine C_{hyd} yields estimates of C_{el} that are mostly negative. In the case of the normal alcohol solvents, the observed coupling parameters are much less than those predicted on the basis of ζ_{el}/ζ_{stick}.

What can be concluded from these comparisons regarding the applicability of dielectric friction ideas? To answer this question, it is helpful to examine the magnitudes of the dielectric friction effects predicted on the basis of eq 7. Consider first the polar aprotic solvents. Comparing the values of C_{el} and C_{obs} provided in Table 1, one finds that the predicted dielectric friction effect on the coupling parameter is a relatively small fraction of C_{obs}. For this class of solvents (and also for the protic solvents other than the *n*-alcohols) C_{el}/C_{obs} averages only ~15%, with few solvents showing values larger than 25%. These numbers can be compared to the variations in the coupling parameters observed in different nonpolar solvents. In these solvents we have noted a primary correlation between C_{obs} and the solvent/solute size ratio ρ. But individual solvents show deviations $(C_{np}(\rho) - C_{obs})/C_{obs}$ from this correlation which average about ±14%. This variability presumably reflects other shape/interaction features not accounted for by solvent size alone.[96] Since the polar solvents present a more varied collection than the nonpolar solvents, it is likely that these other solvent attributes (whatever they are) would cause a comparable or larger variability among the coupling parameters in polar solvents that would tend to obscure the variations due to dielectric friction effects. Thus, the lack of a good correlation between C_{el} and ζ_{el}/ζ_{stick} in the case of these solvents says little about the correctness of dielectric friction ideas. However, the scatter observed underscores the conclusion that, in most solvents, dielectric friction effects on solutes such as C153 are likely to be smaller than, or at best comparable to, other sources of nonhydrodynamic behavior.

It is only in the case of normal alcohol solvents that dielectric friction effects on rotation are predicted to be large. Among the six *n*-alcohols examined here the average value of C_{el}/C_{obs} is ~165%. These values are well beyond the scatter in the nonpolar solvent data and should therefore be readily observable. However, no large increase in C_{obs} is found for these solvents. In fact, using $C_{np}(\rho)$ to estimate C_{hyd} yields negative values of C_{el} for most of the *n*-alcohols studied. Thus, in the case of the *n*-alcohol solvents, there is clearly something wrong with the basic notion of dielectric friction and its relation to solvation dynamics as embodied in the van der Zwan−Hynes connection (eq 7).

V. Summary and Conclusions

In this study we have employed fluorescence anisotropy measurements with subpicosecond time resolution to study the rotational dynamics of the dipolar solute C153 in a wide range of polar and nonpolar solvents. C153 was chosen partly because it represents an exceptionally well-studied example of a highly dipolar solute (in S_1 $\mu \sim 15$ D[86]) that interacts strongly with polar solvents mainly through nonspecific dipole−dipole forces.[77] The primary objective of this work was to analyze the rotation times of C153 in order to determine what effect these electrical forces, or "dielectric friction", have on its rotational dynamics. In particular, we sought to use the extensive database on polar solvation dynamics accumulated for the C153 probe[70,77] to test the general connection between rotational dielectric friction and solvation dynamics first proposed by van der Zwan and Hynes.[7] The present study is the first to test this connection by comparing solvation and rotational dynamics *measured for the same solute*. In light of the conclusions reached in this most general test, we have not examined analytic theories of dielectric friction here. However, an investigation of the accuracy of the dielectric continuum models employed in such theories (using the same C153 solvation data) is carried out in a separate paper.[41]

A number of unexpected results emerged from this study. The first is the observation that the rotational anisotropy decays of C153 and thus the rotational correlation functions they imply are generally nonexponential functions of time (Figures 3 and 4). Nonexponential anisotropies have seldom been reported for large solutes like C153. When nonexponential behavior is observed, it has normally been attributed to anisotropic rotational motions which result from very different friction constants for rotation about different molecular axes. (Perylene is a well-known example.[97]) In the present case, nonexponential anisotropies do not appear to reflect anisotropic rotational motion. Nor are they a direct manifestation of solvation dynamics as we originally postulated.[72] Rather, the nonexponentiality observed with C153 results from the rotational friction falling outside of the Markovian regime. That is, in many solvents, the time-dependent friction on the rotational motion is not fast enough to lead to purely exponential rotational decays. To our knowledge, nonexponential rotational anisotropies having this origin have not been previously reported.[98] But, such behavior should probably not be viewed as an anomaly. It is probably the case that our use of multiple time steps and good signal-to-noise ratio in these measurements enabled observation of what may be a common phenomenon in molecules the size of C153. By fitting the nonexponential anisotropies to biexponential model friction functions (eq 14, Table 2), it is possible to infer semiquantitative information about the time dependence of the rotational friction on C153. As expected, such fits show that the friction consists of a dominant fast component (usually >96% amplitude, $\tau < 1$ ps) together with a small-amplitude, slow component. The time constants of the slow component are all remarkably close to the slowest time constants observed in solvation dynamics measurements. However, this slowest dynamics is represented to an extent that is roughly an order of magnitude smaller in the rotational friction than in the solvation response (Table 2).

The primary results of this work concern the solvent dependence of the average rotation times, which are directly related to the integral friction on the rotational motion (eq 16). Viewing these average rotation times as a function of viscosity (Figure 6), one finds that there is a marked difference between the behavior of C153 in nonpolar (alkane) and polar solvents. C153 rotates considerably faster in nonpolar solvents than in polar solvents of comparable viscosity. The two classes of solvents also show distinct correlations with viscosity. In the case of polar solvents rotation times are simply proportional to viscosity, whereas in nonpolar solvents the relationship is of a power law $\langle\tau\rangle_{rot} \propto \eta^{\rho}$ with $\rho \cong 0.6$. Another important observation is that hydrogen-bond-donating and polar aprotic

solvents behave in an indistinguishable manner as far as these viscosity correlations are concerned. Thus, in contrast to previous conjectures concerning rotation of such molecules,[75] the rotational dynamics of C153 appears to be relatively unaffected by specific associations with hydrogen-bonding solvents. Collectively, these observations suggest that the "excess" rotation times of C153 in polar solvents compared to isoviscous nonpolar reference solvents might be ascribed to the operation of dielectric friction. However, attempts to correlate these excess times with the magnitudes of dielectric friction predicted from solvation dynamics data (via eq 7) proved unsuccessful (Figure 7). Rather than polarity being the key factor differentiating these two classes of solvents, it seems more important that for a given viscosity nonpolar solvents are larger.

Contrary to expectations, the rotation times of C153 in both polar and nonpolar solvents can be interpreted primarily in terms of a decreasing solute−solvent coupling with increasing solvent size (Figure 8). This nonhydrodynamic effect is most apparent in the nonpolar solvents, where the solvent size varies widely. It provides a satisfying explanation for the power-law relation between the rotation times and viscosity observed in these solvents. As previously noted, such size effects are not unique to C153. Similar effects have been observed in a number contexts previously, mainly with nonpolar solutes,[46,82,83,89−93] and it seems likely that this size dependence is a general phenomenon. Some indication of this generality is provided by the comparison (Figure 9) between the data collected here on C153 and data compiled on the rotation times of 16 assorted solutes in the single solvent *n*-hexane.[89] At least for these two sets of data, we observe what appears to be a single, relatively simple correlation between the rotational coupling parameter and the solvent/solute size ratio ρ. The relationship can be approximately expressed $(1/C_{obs} - 1) \propto \rho^{3/2}$. A number of theories of rotational friction predict a dependence of the coupling parameter on ρ of this general sort. As in previous experimental studies,[46,83,89−93] we compared experimental results to the predictions of two of these theories, due to Gierer and Wirtz[24] and to Dote, Kivelson, and Schwartz (DKS).[25] While neither theory provides predictions in quantitative agreement with experiment, the Geirer−Wirtz theory comes close to predicting the proper form of the ρ dependence. The more sophisticated DKS theory predicts a dependence on ρ that is much weaker than observed experimentally.[95] This apparent failure of the DKS model is disappointing given the fact that it represents the most advanced model currently available that affords simple comparison to experiment.

It is important to realize that, even within the class of alkane solvents considered here, solvent size is not the only determinant of C_{obs}. Thus, the scatter about the single-variable correlation between C_{obs} and ρ illustrated in Figure 9 averages ±14%. Individual solvents can show much larger variations. For example, in cyclohexane, the deviation between the observed coupling and that predicted on the basis of the remaining solvents is as much as 50%. Presumably, such deviations reflect the influence of solvent shape and possibly other factors on the frictional coupling. Given the wealth of experimental information available in the literature, more could probably be learned through attempts to correlate C_{obs} with more sophisticated solvent/solute properties. Success in this endeavor would provide empirical guidance for improving theoretical models.[99] We are currently pursuing this approach.

For the present, we note that the interesting variability of C_{obs} found even among nonpolar solvents undermines the use of the solvent dependence of rotation times as a means of determining the effects of dielectric friction in polar solvents. In the case of C153 it appears that approximately the same correlation between C_{obs} and ρ holds for both polar and nonpolar solvents alike. Thus, it seems that this size effect rather than dielectric friction is the primary cause of the dramatic difference between the rotation times observed in the two classes of solvents. Once this dominant influence of solvent size is approximately accounted for, the residual variations in C_{obs} are no larger than the scatter of the nonpolar solvent data. There is no clear correlation between the variations of C_{obs} derived in this manner and predicted dielectric friction magnitudes. Thus, we cannot claim that we have observed any manifestation of dielectric friction in the present experiments. Part of the problem is that we have fallen slightly short of the "ideal" experiment described in section II. While the present experiments incorporate many of the necessary features required for providing stringent tests of dielectric friction ideas, their one major drawback is that we have only measured rotational dynamics in one electronic state of the probe. If rotation times in both the S_0 and S_1 states were available, examining the S_1-S_0 differences in a given solvent would obviate the difficulties inherent in measuring the dielectric friction effect by comparing chemically different solvents (or solutes). We are hoping that we will be able to accomplish more exacting tests using C153 or similar probes in future work.[100]

Some conclusions regarding dielectric friction can nevertheless be drawn from the present work. In polar aprotic solvents, and in many protic solvents as well, the effect of nonspecific dielectric friction on the rotation of uncharged molecules is predicted to be quite small. Even in the case of the S_1 state of C153, which has a 15 D dipole moment, the dielectric component of the rotational friction is predicted to account for only 10−20% of C_{obs}. Thus, in most solvents, to confidently conclude that one has observed the effects of dielectric friction probably does require measurements of a single solvent/solute pair in different solute electronic states. Of the solvents studied here, the only exceptions to this small predicted effect are the normal alcohols. In these solvents, dielectric friction is expected to have a large influence on rotation times, much larger than the scatter in the remaining data. At least for these solvents, there appears to be a clear discrepancy between the observed rotation times and the general expectations of dielectric friction theory.[101] The large dielectric effects that should result from the exceptionally slow solvation times of the normal alcohols are somehow not manifest in the rotational motion. It is not that such solvation components are not present in the friction. The results of fitting $r(t)$ to model friction functions clearly show that slow components are indeed present in the time-dependent friction. As already mentioned, the approximate times deduced for these components bear an uncanny resemblance to the slowest solvation times in the *n*-alcohol solvents. However, the effect of these slow components on the total friction is much smaller than anticipated.[102] To understand why this is the case further experiments of the sort discussed above would be helpful. Computer simulations of realistic solute/solvent combinations should be even more helpful in testing and refining our understanding of dielectric friction. The simulations that have recently appeared[80,103] and those ongoing in our laboratory[40] point to one likely reason for the failure of dielectric friction modeling. They indicate that the coupling between dielectric and hydrodynamic components of the friction may be too important to allow for easy separations of the sort used in current analysis (i.e., for the validity of eq 4). Some basic revision of our thinking about the nature of dielectric friction may be required before further progress can be made in this area.

To conclude, the present results on C153 underscore the fact that we are far from having a complete understanding of how it is that the molecular details of solute−solvent interactions translate into friction on solute motion. In nonpolar solvents, existing theories provide only qualitative guidance with respect to the rotational dynamics observed with molecules such as C153. In polar solvents the situation is worse. Here the qualitative ideas of dielectric friction in current use may not even provide a correct first-order description of how polar interactions modify the friction. Since the concept of friction is central to any description of dynamics (i.e., chemical reaction) in solution, this situation is unsatisfying to say the least. We hope that the results provided by this and similar experiments will encourage more theoretical interest in treating this old but central problem in solution phase chemistry.

Acknowledgment. The authors thank Mark P. Heitz for making time-correlated single-photon-counting measurements of long-time rotational dynamics of C153 in some of the slowest solvents. Financial support of this work was provided by the Office of Basic Energy Sciences of the U.S. Department of Energy and made possible through instrumentation provided by the Office of Naval Research.

References and Notes

(1) References 2−4 contain useful overviews on various aspects of the subject of rotational dynamics.

(2) *Rotational Dynamics of Small and Macromolecules*, 4th ed., Dorfmuller, T., Pecora, R., Eds.; Springer-Verlag: Berlin, 1987; Vol. 293. See especially the excellent introductory chapter by D. Kivelson, p 1.

(3) Boere, R. T.; Kidd, R. G. *Annu. Rep. Prog. NMR Spectrosc.* **1982**, *13*, 319.

(4) Fleming, G. R. *Chemical Applications of Ultrafast Spectroscopy*; Oxford: New York, 1986; Section 6.2.

(5) See, for example, the reviews: Hynes, J. T. In *Ultrafast Dynamics of Chemical Systems*; Simon, J. D., Ed.; Klewer: Dordrecht, 1994; p 345. Voth, G. A.; Hochstrasser, R. M. *J. Phys. Chem.* **1996**, *100*, 13034.

(6) Debye, P. *Polar Molecules*; Chemical Catalog Co.: New York, 1929.

(7) van der Zwan, G.; Hynes, J. T. *J. Phys. Chem.* **1985**, *89*, 4181.

(8) Some authors write eq 2a so that it includes a viscosity-independent term τ_0 that allows for a nonzero intercept in the relationship between rotation times and η/T. While such an intercept is often needed to adequately fit rotation times of small solutes to a (linear) function of η/T, the theoretical interpretation of this term, often mistakenly referred to as the "free rotor time", is not clear.[9] Since the experimental data described here do not require the presence of such a nonzero intercept, we prefer to ignore this additional term in our discussions.

(9) Evans, G. T.; Kivelson, D. *J. Chem. Phys.* **1986**, *84*, 385.

(10) Perrin, F. *Phys. Radium* **1934**, *5*, 497.

(11) The physical meaning of this factor (sometimes symbolized by κ) is nicely discussed in the paper: Kivelson, D.; Kowert, B. *J. Chem. Phys.* **1976**, *64*, 5206.

(12) Exceptions may arise in the case of supercooled liquids. See, for example: Tarjus, G.; Kivelson, D. *J. Chem. Phys.* **1995**, *103*, 3071.

(13) Zwanzig, R.; Harrison, A. K. *J. Chem. Phys.* **1985**, *83*, 5861.

(14) Hu, C.-M.; Zwanzig, R. *J. Chem. Phys.* **1974**, *60*, 4354.

(15) Youngren, G. K.; Acrivos, A. *J. Chem. Phys.* **1975**, *63*, 3846. See also the clarifying comment: Sension, R. J.; Hochstrasser, R. M. *J. Chem. Phys.* **1993**, *98*, 2490.

(16) Ahn, M. K. *Chem. Phys. Lett.* **1977**, *52*, 135.

(17) Zwanzig, R. *J. Chem. Phys.* **1978**, *68*, 4325.

(18) Kivelson, D. In ref 2.

(19) Bauer, D. R.; Alms, G. R.; Brauman, J. I.; Pecora, R. *J. Chem. Phys.* **1974**, *61*, 2255. Bauer, D. R.; Brauman, J. I.; Pecora, R. *J. Am. Chem. Soc.* **1974**, *96*, 6840.

(20) Williams, A. M.; Jiang, Y.; Ben-Amotz, D. *Chem. Phys.* **1994**, *180*, 119. Ben-Amotz, D.; Scott, T. W. *J. Chem. Phys.* **1987**, *87*, 3739.

(21) Chandler, D. *J. Chem. Phys.* **1974**, *60*, 3508.

(22) Hynes, J. T., Kapral, R.; Weinberg, M. *J. Chem. Phys.* **1978**, *69*, 2725. Hynes, J. T.; Kapral, R.; Weinberg, M. *J. Chem. Phys.* **1977**, *67*, 3256.

(23) Evans, G. T. *J. Chem. Phys.* **1989**, *91*, 1252. Evans, G. T. *J. Chem. Phys.* **1988**, *88*, 5035. Evans, G. T.; Cole, R. G.; Hoffman, D. K. *J. Chem. Phys.* **1982**, *77*, 3209.

(24) Gierer, A.; Wirtz, K. *Z. Naturforsch.* **1953**, *A8*, 532.

(25) Dote, J. L.; Kivelson, D.; Schwartz, R. N. *J. Phys. Chem.* **1981**, *85*, 2169.

(26) Ravi, R.; Ben-Amotz, D. *Chem. Phys.* **1994**, *183*, 385.

(27) This terminology comes from it use in studies of ion mobilities. Much of the important literature in this area was reviewed in: Wolynes, P. G. *Annu. Rev. Phys. Chem.* **1980**, *31*, 345, which also provides a helpful discussion of the nature of the two limiting cases.

(28) Detailed calculations of rotational motion based on this solventberg idea were first discussed in: Spears, K. G.; Steinmetz, K. M. *J. Phys. Chem.* **1985**, *89*, 3623.

(29) Useful reviews of continuum dielectric theories of rotational dielectric friction can be found in the articles: Papazyan, A.; Maroncelli, M. *J. Chem. Phys.* **1995**, *102*, 2888. Alavi, D. S.; Hartman, R. S.; Waldeck, D. H. *J. Chem. Phys.* **1991**, *94*, 4509. A review of recent molecular theories is: Ravichandran, S.; Bagchi, B. *Int. Rev. Phys. Chem.* **1995**, *14*, 271.

(30) Nee, T. W.; Zwanzig, R. *J. Chem. Phys.* **1970**, *52*, 6353.

(31) Hubbard, J. B.; Wolynes, P. G. *J. Chem. Phys.* **1978**, *69*, 998.

(32) Brito, P.; Bordewijk, P. *Mol. Phys.* **1980**, *39*, 217.

(33) Madden, P.; Kivelson, D. *J. Phys. Chem.* **1982**, *86*, 4244.

(34) van der Zwan, G.; Hynes, J. T. *Physica* **1983**, *121A*, 227.

(35) Alavi, D. S.; Waldeck, D. H. *J. Chem. Phys.* **1991**, *94*, 6196. Alavi, D. S.; Waldeck, D. H. *J. Chem. Phys.* **1993**, *98*, 3580.

(36) Hubbard, J. B. *J. Chem. Phys.* **1978**, *69*, 1007.

(37) Felderhof, B. U. *Mol. Phys.* **1983**, *48*, 1269. Felderhof, B. U. *Mol. Phys.* **1983**, *48*, 1283.

(38) Nowak, E. *J. Chem. Phys.* **1983**, *79*, 976.

(39) Actually, in more sophisticated "electrohydrodynamic" theories of dielectric friction of the sort discussed in refs 37−39 hydrodynamic and electrostatic friction are not purely additive as they are in the simpler theories.[31−36] However, the separation is still useful for conceptual purposes.

(40) Simulations of small diatomics in acetonitrile and methanol solvents show that as one increases the charges on solute atoms the hydrodynamic part of the friction increases dramatically due to "electrostriction" effects. This increase is in fact the primary source of the extra friction on dipolar versus nondipolar solutes. (Kumar, V. P.; Maroncelli, M. Manuscript in preparation.)

(41) Maroncelli, M. Continuum Estimates of Rotational Dielectric Friction and Polar Solvation. *J. Chem. Phys.*, in press.

(42) Papazyan, A.; Maroncelli, M. *J. Chem. Phys.* **1995**, *102*, 2888. See also: Ravichandran, S.; Roy, S.; Bagchi, B. *J. Phys. Chem.* **1995**, *99*, 2489.

(43) The assumption is also made that the solute's rotational motion is sufficiently slow relative to the solvent dynamics that the effect of the probe rotation can be ignored. This assumption should be reasonably accurate for large solutes such as C153 but might be inappropriate for much smaller solutes. (This decoupling assumption enables use of the electric field correlation function to describe the *random* part of the torque autocorrelation function which appears in the expression for the rotational friction. See ref 42 for more discussion and tests of this approximation.)

(44) Reviews on the subject of polar solvation dynamics and its measurement via time-resolved emission spectroscopy can be found in: Stratt, R. M.; Maroncelli, M. *J. Phys. Chem.* **1996**, *100*, 12981. Maroncelli, M. *J. Mol. Liq.* **1993**, *57*, 1. Barbara, P. F.; Jarzeba, W. *Adv. Photochem.* **1990**, *15*, 1.

(45) Philips, L. A.; Webb, S. P.; Clark, J. H. *J. Chem. Phys.* **1985**, *83*, 5810.

(46) Nakahara, M.; Emi, K. *J. Chem. Phys.* **1993**, *99*, 5418. Ibuki, K.; Nakahara, M. *J. Chem. Phys.* **1989**, *90*, 386. Nakahara, M.; Ibuki, K. *J. Chem. Phys.* **1986**, *85*, 4654.

(47) Gudgin Templeton, E. F.; Kenney-Wallace, G. A. *J. Phys. Chem.* **1986**, *90*, 5441. Gudgin Templeton, E. F.; Kenney-Wallace, G. A. *J. Phys. Chem.* **1986**, *90*, 2896. Gudgin Templeton, E. F.; Quitevis, E. L.; Kenney-Wallace, G. A. *J. Phys. Chem.* **1985**, *89*, 3238.

(48) Blanchard, G. J. *J. Phys. Chem.* **1989**, *93*, 4315.

(49) Simon, J. D.; Thompson, P. A. *J. Chem. Phys.* **1990**, *92*, 2891.

(50) Dutt, G. B.; Doraiswamy, S.; Periasamy, N.; Venkataraman, B. *J. Chem. Phys.* **1990**, *93*, 8498. Dutt, G. B.; Doraiswamy, S. In *Ultrafast Processes in Spectroscopy*; IOP Publishing: Philadelphia, PA, 1992; Vol. 531. Dutt, G. B.; Doraiswamy, S. *J. Chem. Phys.* **1992**, *96*, 2475. Dutt, G. B.; Doraiswamy, S.; Periasamy, N. *J. Chem. Phys.* **1991**, *94*, 5360.

(51) Srivastava, A.; Doraiswamy, S. *J. Chem. Phys.* **1995**, *103*, 6197.

(52) Bushuk, B. A.; Rubinov, A. N.; Berestov, A. L. *Sov. J. Chem. Phys.* **1991**, *8*, 2629.

(53) Vauthey, E. *Chem. Phys. Lett.* **1993**, *216*, 530.

(54) Harju, T. O.; Erostyak, J.; Chow, Y. L.; Korppi-Tommola, J. E. I. *Chem. Phys.* **1994**, *181*, 259.

(55) Bessire, D. R.; Quitevis, E. L. *J. Phys. Chem.* **1994**, *98*, 13083. Quitevis, E. L.; Horng, M.-L. *J. Phys. Chem.* **1990**, *94*, 5684.

(56) Levitus, M.; Negri, R. M.; Aramendia, P. F. *J. Phys. Chem.* **1995**, *99*, 14231.

(57) Imeshev, G.; Khundkar, L. R. *J. Chem. Phys.* **1995**, *103*, 8322.

(58) Alavi, D. S.; Waldeck, D. H. *J. Phys. Chem.* **1991**, *95*, 4848.

(59) Alavi, D. S.; Hartman, R. S.; Waldeck, D. H. *J. Chem. Phys.* **1991**, *94*, 4509.

(60) Alavi, D. S.; Hartman, R. S.; Waldeck, D. H. *J. Chem. Phys.* **1991**, *95*, 6770.

(61) Hartman, R. S.; Alavi, D. S.; Waldeck, D. H. *J. Phys. Chem.* **1991**, *95*, 7872.

(62) Hartman, R. S.; Waldeck, D. H. *J. Phys. Chem.* **1994**, *98*, 1386.

(63) Hartman, R. S.; Konitsky, W. M.; Waldeck, D. H.; Chang, Y. J.; Castner, E. W., Jr. "Probing Solute−Solvent Electrostatic Interactions. Rotational Diffusion Studies of 9,10-Disubstituted Anthracenes. Submitted to *J. Phys. Chem.*

(64) For example, the data reported by Blanchard (Blanchard, G. J. *J. Phys. Chem.* **1988**, *92*, 6303) were first interpreted by Blanchard in terms of solvent attachment and then reinterpreted in terms of nonspecific dielectric friction effects by Simon and Thompson in ref 49. (See also the further discussion in: Blanchard, G. J. *J. Phys. Chem.* **1991**, *95*, 5293.)

(65) Blanchard, G. J.; Cihal, C. A. *J. Phys. Chem.* **1988**, *92*, 5950.

(66) An overview of much of this work can be found in the review: Hartman, R. S.; Alavi, D. S.; Waldeck, D. H. *Isr. J. Chem.* **1993**, *33*, 157.

(67) Lakowicz, J. R. *Principles of Fluorescence Spectroscopy*; Plenum Press: New York, 1983.

(68) Shinitzky, M.; Dianoux, A. C.; Gilter, C.; Weber, G. *Biochemistry* **1971**, *10*, 2106.

(69) Riddick, J. A.; Bunger, W. B.; Sakano, T. K. *Organic Solvents*; Wiley: New York, 1986.

(70) Horng, M. L.; Gardecki, J. A.; Papazyan, A.; Maroncelli, M. *J. Phys. Chem.* **1995**, *99*, 17311.

(71) Blanchard and co-workers [Jiang, Y.; McCarthy, P. K.; Blanchard, G. J. *Chem. Phys.* **1994**, *183*, 249] have hypothesized that multiple emitting states complicate the emission of C153. Based on these anisotropy results and a number of other features of the spectroscopy of C153 reported in ref 70, such a possibility seems very unlikely. (See note 79 of ref 70 for further discussion.)

(72) Maroncelli, M.; Fleming, G. R. *J. Chem. Phys.* **1987**, *86*, 6221; *J. Chem. Phys.* **1990**, *92*, 3251.

(73) Bevington, P. R. *Data Reduction and Error Analysis for the Physical Sciences*; McGraw-Hill: New York, 1969.

(74) These measurements were carried out using a Ti:sapphire-based system. The electronic detection and analysis methods were similar to those reported in ref 75, except that the time resolution of the instrument employed here (∼25 ps fwhm instrument response function) was considerably better than in the previous studies.

(75) Moog, R. S.; Bankert, D. L.; Maroncelli, M. *J. Phys. Chem.* **1993**, *97*, 1496.

(76) Edwards, J. T. *J. Chem. Educ.* **1970**, *47*, 261.

(77) Reynolds, L.; Gardecki, J. A.; Frankland, S. J. V.; Horng, M. L.; Maroncelli, M. *J. Phys. Chem.* **1996**, *100*, 10337.

(78) Chuang, T. J.; Eisenthal, K. B. *J. Chem. Phys.* **1972**, *57*, 5094. Tao, T. *Biopolymers* **1969**, *8*, 609.

(79) Reference 42 uses simulations of a simple solvent model to explore the nature of rotational correlation functions and the manifestations of non-Markovian friction. See this work for more detailed discussion.

(80) Bruehl, M.; Hynes, J. T. *J. Phys. Chem.* **1992**, *96*, 4068.

(81) We choose to use an exponential function for the faster component here rather than a (more realistic) Gaussian function due to the greater ease of performing the inverse Laplace transformation required to obtain $C_r(t)$ from $\zeta(t)$.

(82) Goulay-Bize, A. M.; Dervil, E.; Vincent-Geisse, J. *Chem. Phys. Lett.* **1980**, *69*, 319. Canonica, S.; Schmid, A. A.; Wild, U. P. *Chem. Phys. Lett.* **1985**, *122*, 529. Lee, M.; Bain, A. J.; McCarthy, P. J.; Han, C. H.; Haseltine, J. N.; Smith, I. I. I.; Hochstrasser, R. M. *J. Chem. Phys.* **1986**, *85*, 4341. Bowman, R. M.; Eisenthal, K. B. *Chem. Phys. Lett.* **1989**, *155*, 99. Brocklehurst, B.; Young, R. N. *J. Phys. Chem.* **1995**, *99*, 40.

(83) Kim, S. K.; Fleming, G. R. *J. Phys. Chem.* **1988**, *92*, 2168

(84) Lewis, J. A.; Maroncelli, M. Unpublished results of calculations using a number of semiempirical Hamiltonians.

(85) Pastor, R. W.; Zwanzig, R. *J. Chem. Phys.* **1989**, *90*, 5729. Venable, R. M.; Pastor, R. W. *Biopolymers* **1988**, *27*, 1001.

(86) Baumann, W.; Nagy, Z. *Pure Appl. Chem.* **1993**, *65*, 1729. Baumann, W.; Nagy, Z.; Maiti, A. K.; Reis, H.; Rodrigues, S. V.; Detzer, N. In *Dynamics and Mechanisms of Photoinduced Electron Transfer and Related Phenomena*; Mataga, N., Okada, T., Masuhara, H., Eds.; Elsevier: Amsterdam, 1992; p 211.

(87) Kumar, V. P.; Maroncelli, M. Unpublished results.

(88) Moylan, C. R. *J. Phys. Chem.* **1994**, *98*, 13513.

(89) Ben-Amotz, D.; Drake, J. M. *J. Chem. Phys.* **1988**, *89*, 1019. See also ref 26.

(90) Roy, M.; Doraiswamy, S. *J. Chem. Phys.* **1993**, *98*, 3213.

(91) Akesson, E.; Hakkarainen, A.; Laitnen, E.; Helenius, V.; Gilbro, T.; Korppi-Tommola, J.; Sundstrom, V. *J. Chem. Phys.* **1991**, *95*, 6508.

(92) Anderton, R. M.; Kauffman, J. F. *J. Phys. Chem.* **1994**, *98*, 12117.

(93) De Backer, S.; Dutt, G. B.; Ameloot, M.; De Schryver, F. C.; Mullen, K.; Holtrup, F. *J. Phys. Chem.* **1996**, *100*, 512.

(94) See for example, Frenkel, J. *Kinetic Theory of Liquids*; Dover: New York, 1955.

(95) Our statements here concerning the applicability of the DKS theory are largely confined to the C153 data set. If the DKS theory were to be applied to the collected solute data also shown in Figure 9, the factor of ϕ in eq 22a would vary somewhat with the solute shape. If this variation were correlated to the solute size, it could lead to a different overall dependence on ρ than the one displayed here.

(96) One notable example of this variability is the difference between the solvents *n*-hexane ($C_{obs} = 0.46$) and cyclohexane ($C_{obs} = 0.34$), which have nearly the same volume. This difference is also observed with solutes other than C153.

(97) See for example: Christensen, R. L.; Drake, R. C.; Phillips, D. *J. Phys. Chem.* **1986**, *90*, 5960. Barkley, M. D.; Kowalczyk, A. A.; Brand, L. *J. Chem. Phys.* **1981**, *75*, 3581 and references therein.

(98) Waldeck and co-workers did ascribe nonexponential anisotropy decays observed with a phenoxazine dye in 2-propanol to this origin[60] but later determined the source of the nonexponentiality was inhomogeneity of the samples caused by the presence of water.[66]

(99) We note that Ben-Amotz and co-workers[20,89] have already provided very useful compilations of much of the rotational data available up to 1993 and have drawn a number of useful conclusions about solute−solvent coupling on the basis of these data. However, we believe that a more detailed analysis of the solvent dependence of the data in alkane solvents might afford additional insights.

(100) Waldeck, D.; Maroncelli, M. Work in progress.

(101) Of course, it is possible that the alcohols do exhibit a significant dielectric friction effect. but that is hidden by a hydrodynamic friction contribution that is much smaller than expected. Some evidence for this interpretation can be made from the observation of subslip dynamics for many nonpolar solutes in alcohols.[20] Again, measurements of rotational dynamics in two electronic states of the same solute would prove helpful in testing this possibility. However, for now we note that the similarity in the behavior in alcohol and other polar solvents makes such an interpretation appear unlikely.

(102) As can be seen from Table 2 ("%ζ" column), the effect of these long-time components on the friction constant is far from small. It is ∼50% of the total friction in the *n*-alcohols. If all of this long component were associated solely with ζ_{el}, the ratio of ζ_{el}/ζ_{tot} would be about what dielectric friction theories predict. However, a large part of this slower friction component can probably be attributed to ζ_{hyd}.

(103) Kurnikova, M. G.; Waldeck, D. H.; Coalson, R. D. *J. Chem. Phys.* **1997**, *105*, 628.